

ϕ-Meson production at forward rapidity in p-Pb collisions at $\sqrt{S_NN}$=5.02 TeV and in pp collisions at $\sqrt{S}$=2.76 TeV

J-L. Charvet, V.J.G. Feuillard, A. Rakotozafindrabe, J. Adam, Laurent Aphecetche, B. Audurier, A. Baldisseri, H. Borel, J. Castillo Castellanos, C. Cheshkov, et al.

▶ **To cite this version:**

J-L. Charvet, V.J.G. Feuillard, A. Rakotozafindrabe, J. Adam, Laurent Aphecetche, et al.. ϕ-Meson production at forward rapidity in p-Pb collisions at $\sqrt{S_NN}$=5.02 TeV and in pp collisions at $\sqrt{S}$=2.76 TeV. Physics Letters B, 2017, 768, pp.203-217. 10.1016/j.physletb.2017.01.074 . in2p3-01170083v2

HAL Id: in2p3-01170083
https://cea.hal.science/in2p3-01170083v2

Submitted on 31 May 2017

HAL is a multi-disciplinary open access archive for the deposit and dissemination of scientific research documents, whether they are published or not. The documents may come from teaching and research institutions in France or abroad, or from public or private research centers.

L'archive ouverte pluridisciplinaire **HAL**, est destinée au dépôt et à la diffusion de documents scientifiques de niveau recherche, publiés ou non, émanant des établissements d'enseignement et de recherche français ou étrangers, des laboratoires publics ou privés.

Physics Letters B 768 (2017) 203–217

Contents lists available at ScienceDirect

Physics Letters B

www.elsevier.com/locate/physletb

ϕ-Meson production at forward rapidity in p–Pb collisions at $\sqrt{s_{\rm NN}} = 5.02$ TeV and in pp collisions at $\sqrt{s} = 2.76$ TeV

ALICE Collaboration *

ARTICLE INFO

Article history:
Received 16 November 2015
Received in revised form 8 December 2016
Accepted 9 January 2017
Available online 16 February 2017
Editor: L. Rolandi

ABSTRACT

The first study of ϕ-meson production in p–Pb collisions at forward and backward rapidity, at a nucleon–nucleon centre-of-mass energy $\sqrt{s_{\rm NN}} = 5.02$ TeV, has been performed with the ALICE apparatus at the LHC. The ϕ-mesons have been identified in the dimuon decay channel in the transverse momentum ($p_{\rm T}$) range $1 < p_{\rm T} < 7$ GeV/c, both in the p-going ($2.03 < y < 3.53$) and the Pb-going ($-4.46 < y < -2.96$) directions — where y stands for the rapidity in the nucleon–nucleon centre-of-mass — the integrated luminosity amounting to 5.01 ± 0.19 nb^{-1} and 5.81 ± 0.20 nb^{-1}, respectively, for the two data samples. Differential cross sections as a function of transverse momentum and rapidity are presented. The forward–backward ratio for ϕ-meson production is measured for $2.96 < |y| < 3.53$, resulting in a ratio ~ 0.5 with no significant $p_{\rm T}$ dependence within the uncertainties. The $p_{\rm T}$ dependence of the ϕ nuclear modification factor $R_{\rm pPb}$ exhibits an enhancement up to a factor 1.6 at $p_{\rm T} = 3$–4 GeV/c in the Pb-going direction. The $p_{\rm T}$ dependence of the ϕ-meson cross section in pp collisions at $\sqrt{s} = 2.76$ TeV, which is used to determine a reference for the p–Pb results, is also presented here for $1 < p_{\rm T} < 5$ GeV/c and $2.5 < y < 4$, for a 78 ± 3 nb^{-1} integrated luminosity sample.

© 2017 The Author(s). Published by Elsevier B.V. This is an open access article under the CC BY license (http://creativecommons.org/licenses/by/4.0/). Funded by SCOAP[3].

1. Introduction

Proton–nucleus (p–A) collisions are of special interest in the context of high-energy nuclear physics for two reasons. On one hand, a precise characterisation of particle production processes in p–A collisions is needed as a reference for nucleus–nucleus data. This allows in-medium effects — linked to the formation of a deconfined phase of the QCD matter, the quark–gluon plasma (QGP) [1–3] — to be disentangled from the effects already present in cold nuclear matter. Among them, a sizeable role is played by the transverse momentum broadening of initial-state partons due to multiple scattering inside the nucleus, responsible for the Cronin effect [4], which may lead to an enhancement of intermediate-$p_{\rm T}$ hadron spectra. In addition, p–A collisions at LHC energies provide a way to probe the parton distributions of the colliding nucleus at small values of Bjorken-x, in a regime where parton densities can reach saturation [5,6]. In particular, the smallest x values contributing to the wave function of the colliding nucleus can be probed by looking at particle production at large rapidities, in the p-going direction. Such a measurement can thus extend towards lower x-values the results of the lower-energy measurements by the PHOBOS and BRAHMS experiments at RHIC [7,8]. Measurements of identified particle production may, in particular, provide useful constraints for forthcoming theoretical studies of the saturation mechanism at small x.

We have already reported results on charged particle production in p–Pb collisions at mid-rapidity. These results focused on the pseudorapidity density [9] and the $p_{\rm T}$ dependence of the nuclear modification factor [10–12]; the latter was found to be consistent with unity for $p_{\rm T} \gtrsim 2$ GeV/c. The nuclear modification factor of charged hadrons was also studied by the BRAHMS and PHOBOS Collaborations in d–Au collisions at the nucleon–nucleon centre-of-mass energy $\sqrt{s_{\rm NN}} = 200$ GeV at RHIC [13,14], as a function of pseudorapidity, where values smaller than unity were found for $\eta \gtrsim 1$, corresponding to the d-going direction.

In this Letter we report the measurement of ϕ-meson production at forward rapidity in p–Pb collisions at $\sqrt{s_{\rm NN}} = 5.02$ TeV in the transverse momentum ($p_{\rm T}$) range $1 < p_{\rm T} < 7$ GeV/c, for the centre-of-mass rapidity (y) ranges $2.03 < y < 3.53$ (p-going direction) and $-4.46 < y < -2.96$ (Pb-going direction), in the dimuon decay channel with the ALICE detector. This measurement extends the investigation of light-flavour particle production to forward rapidity. At the same time, it represents an essential baseline for the understanding of ϕ production in heavy-ion collisions, where an enhancement of strange particle yields relative to the ones measured in pp collisions has been proposed long ago as a signature of the formation of a QGP phase [15–17] triggering an intense experimental effort already at SPS and RHIC energies [18–24]. It should

* *E-mail address:* alice-publications@cern.ch.

http://dx.doi.org/10.1016/j.physletb.2017.01.074
0370-2693/© 2017 The Author(s). Published by Elsevier B.V. This is an open access article under the CC BY license (http://creativecommons.org/licenses/by/4.0/). Funded by SCOAP[3].

be noted that, despite its hidden strangeness, producing a ϕ-meson in a hadronic collision still implies the creation of a $s\bar{s}$ pair as it is the case for other strange hadrons, even if the hadronisation mechanisms can differ in reason of the different quark composition. In this context, the p–Pb data presented here will provide an important reference for future measurements in Pb–Pb collisions in the LHC Run 2, which will be performed at a comparable energy.

The differential ϕ-meson cross section as a function of transverse momentum is also presented for pp collisions at $\sqrt{s} = 2.76$ TeV. This measurement complements the ALICE results on ϕ-meson production in pp collisions at $\sqrt{s} = 7$ TeV, already reported in [25] and, combined with the latter, is used to build the pp reference for the p–Pb measurements presented here.

2. Experimental setup

A full description of the ALICE detector can be found in [26,27]. The results presented in this Letter have been obtained detecting muon pairs with the muon spectrometer, covering the pseudorapidity region $-4 < \eta_{\rm lab} < -2.5$. Here and in the following, the sign of $\eta_{\rm lab}$ is determined by the choice of the LHC reference system. The other detectors relevant for the analysis are the Silicon Pixel Detector (SPD) of the Inner Tracking System (ITS), the V0 detector and the Zero Degree Calorimeters (ZDC).

The elements of the muon spectrometer are a hadron absorber, followed by a set of tracking stations, a dipole magnet, an iron wall acting as muon filter and a set of trigger stations. The hadron absorber is made of carbon, concrete and steel and is placed 0.9 m away from the interaction point. Its total material budget corresponds to 10 hadronic interaction lengths. The dipole magnet provides an integrated magnetic field of 3 T · m in the vertical direction. The muon tracking is provided by five tracking stations, each one composed of two cathode pad chambers. The first two stations are located upstream of the dipole magnet, the third one in the middle of its gap and the last two downstream of it. A 1.2 m thick iron wall, corresponding to 7.2 hadronic interaction lengths, is placed between the tracking and trigger detectors and absorbs the residual secondary hadrons emerging from the hadron absorber. The hadron absorber together with the iron wall stops muons with total momentum lower than ~ 4 GeV/c. The muon trigger detector consists of two stations, each one composed of two planes of resistive plate chambers, installed downstream of the muon filter.

The SPD consists of two silicon pixel layers, covering the pseudorapidity regions $|\eta_{\rm lab}| < 2.0$ and $|\eta_{\rm lab}| < 1.4$ for the inner and outer layer, respectively. It is used for the determination of the primary interaction vertex position. The V0 is composed of two scintillator hodoscopes covering the pseudorapidity regions $2.8 < \eta_{\rm lab} < 5.1$ and $-3.7 < \eta_{\rm lab} < -1.7$. It is used in the definition of the minimum bias trigger signal, and allows the offline rejection of beam-halo and beam-gas interactions to be performed. The ZDC detectors, positioned symmetrically at 112.5 m from the interaction point, are used to clean the event sample by removing beam–beam collisions not originating from nominal LHC bunches.

3. Data selection and signal extraction

The analysis presented in this Letter is based on two data samples, collected by ALICE during the 2013 p–Pb and pp runs at $\sqrt{s_{\rm NN}} = 5.02$ TeV and $\sqrt{s} = 2.76$ TeV, respectively. In this section we present the details of the data selection, as well as the procedure followed for the extraction of the ϕ-meson signal.

3.1. Data selection

The Minimum-Bias (MB) trigger for the considered data sample is given by the logical AND of the signals in the two V0 detectors [28]. Events containing a muon pair are selected by means of a specific dimuon trigger, based on the detection of two muon candidate tracks in the trigger system of the muon spectrometer, in coincidence with the MB condition. Due to the intrinsic momentum cut imposed by the detector, only muons with $p_{\rm T} \gtrsim 0.5$ GeV/c manage to leave a signal in the trigger chambers.

Because of the different energy of the LHC proton and Pb beams ($E_{\rm p} = 4$ TeV, $E_{\rm Pb} = 1.58$ A · TeV), in p–Pb collisions the nucleon–nucleon centre-of-mass moves in the laboratory with a rapidity $y_0 = 0.465$ in the direction of the proton beam. The directions of the proton and Pb beam orbits were inverted during the p–Pb data taking period. This allowed the ALICE muon spectrometer to access two different rapidity regions[1]: the region $2.03 < y < 3.53$ where the proton beam is directed towards the muon spectrometer (p-going direction) and the region $-4.46 < y < -2.96$ where the Pb beam is directed towards the muon spectrometer (Pb-going direction). In the following, these two rapidity ranges are also referred to as "forward" and "backward", respectively. For pp collisions at $\sqrt{s} = 2.76$ TeV the muon spectrometer covers the rapidity region $2.5 < y < 4$.[2]

Background events not coming from beam–beam interactions are rejected by performing an offline selection, based on the requirement that the timing signals from the V0 and ZDC detectors are compatible with a collision occurring in the fiducial interaction region $|z_{\rm vtx}| \lesssim 10$ cm.

The integrated luminosity for the p–Pb data samples was evaluated as $L_{\rm int} = N_{\rm MB}/\sigma_{\rm MB}$, where $N_{\rm MB}$ is the number of MB events corresponding to the analysed triggered events, and $\sigma_{\rm MB}$ the MB trigger cross section. The value of $N_{\rm MB}$ was obtained by averaging the results of two different methods — one based on the ratio of trigger rates and the other based on the offline selection of dimuon events in the MB data sample [29] — while the MB trigger cross sections $\sigma_{\rm MB}$ were measured with a van der Meer scan and found to be 2.09 ± 0.07 b and 2.12 ± 0.07 b, respectively, for the beam configurations corresponding to the forward and backward rapidity coverage of the muon spectrometer [30]. For the pp data sample, the integrated luminosity is calculated with the method described in [31], using as reference the MB trigger cross section $\sigma_{\rm MB} = 47.7 \pm 0.9$ mb, measured in a van der Meer scan [32].

The resulting values of $L_{\rm int}$ for the analysed p–Pb data samples are 5.01 ± 0.19 nb^{-1} and 5.81 ± 0.20 nb^{-1} [29,30] — corresponding to $\sim 24\,000$ and $\sim 26\,000$ reconstructed $\phi \to \mu\mu$ decays (see next section) — respectively for the forward and backward rapidity regions. For the pp data sample, the integrated luminosity amounts to 78 ± 3 nb^{-1} for a total number of $\sim 1\,400$ reconstructed $\phi \to \mu\mu$ decays.

Track reconstruction in the muon spectrometer is based on a Kalman filter algorithm [25,33,34]. Muon identification is performed by requiring the candidate track to match a track segment in the trigger chambers (trigger tracklet). This request selects muons with $p_{{\rm T},\mu} \gtrsim 0.5$ GeV/c and, as a consequence, significantly affects the collected statistics for dimuons with invariant mass $\lesssim 1$ GeV/c^2 and $p_{\rm T} \lesssim 1$ GeV/c. It is also required that muon tracks lie in the pseudorapidity interval $-4 < \eta_\mu < -2.5$, where η_μ is defined in the laboratory frame, in order to remove the tracks close to the acceptance borders of the spectrometer, where the acceptance drops abruptly. Selected tracks are finally required to exit the hadron absorber at a radial distance from the beam axis, $R_{\rm abs}$, in the range $17.6 < R_{\rm abs} < 89.5$ cm: this cut, for all practical purposes equivalent to the one on η_μ, explicitly ensures the rejection

[1] The sign of y is defined by assuming the proton beam to have positive rapidity.
[2] In this case the sign of y is defined by assuming the proton beam entering the muon spectrometer to have positive rapidity.

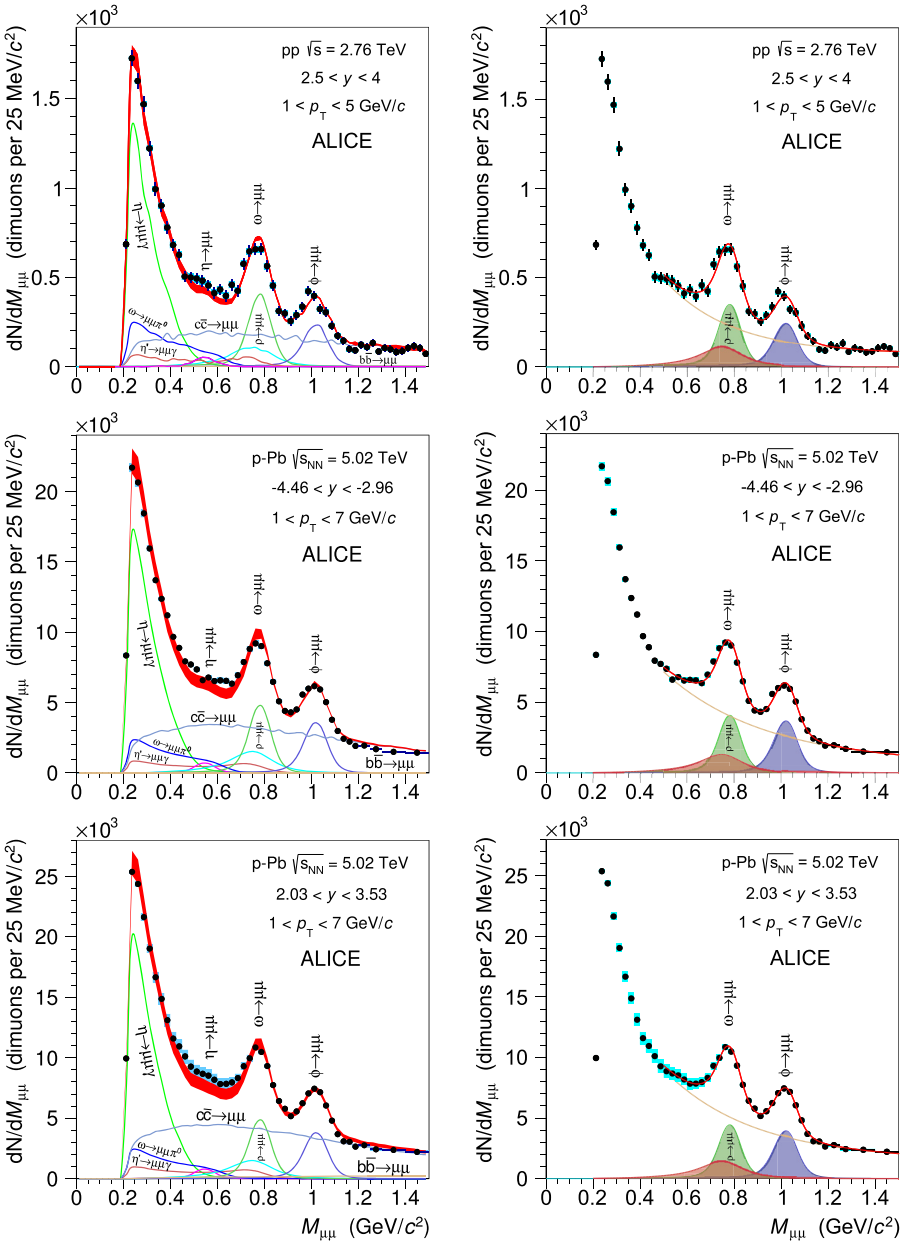


Fig. 1. Dimuon mass spectrum after combinatorial background subtraction: p_T-integrated pp sample (top panels) and p_T-integrated p–Pb sample in the backward (centre panels) and forward (bottom panels) rapidity regions, compared to the result of the hadronic-cocktail and the empirical-function fits (left- and right-column panels, respectively). Error boxes on data points (well visible only in some regions on the plots) represent the systematic uncertainty due to the combinatorial background subtraction, while error bars account for the statistical uncertainty. The width of the hadronic-cocktail fit result (red band) combines the statistical uncertainties of the free fit parameters with the systematic uncertainties on the fixed parameters (see text). (For interpretation of the references to colour in this figure, the reader is referred to the web version of this article.)

of tracks crossing the region of the absorber with the highest density material, where multiple scattering and energy loss effects are large and can affect the mass resolution. Muon pairs are built combining two muon tracks that satisfy the above cuts.

3.2. Signal extraction

The Opposite-Sign (OS) muon pairs are composed of correlated and uncorrelated pairs. The former contain the signal of interest for the present analysis, while the latter — mainly coming from semi-muonic decays of pions and kaons — form a combinatorial background. The contribution of the combinatorial background to the OS mass spectrum was evaluated using an event mixing technique in which uncorrelated pairs are formed with muons taken from different events. A detailed description of the technique can be found in [25]. The ratio between correlated and uncorrelated OS dimuons at the ϕ-meson mass is ~ 0.65 (~ 0.40) in p–Pb collisions at $\sqrt{s_{NN}} = 5.02$ TeV at forward (backward) rapidity, and ~ 1.30 in pp collisions at $\sqrt{s} = 2.76$ TeV. A direct comparison of the raw OS mass spectrum and the associated combinatorial background is presented in [35], for each of the p_T intervals considered in the analysis.

The invariant mass spectra in pp and p–Pb collisions, obtained after combinatorial background subtraction, are shown in Fig. 1 for the p_T-integrated samples. In the left-column panels of Fig. 1, the signal is described in the low-mass region (from the threshold

up to ~ 1.5 GeV/c^2) by the superposition of a so-called hadronic cocktail and the open charm and open beauty processes. The processes included in the hadronic cocktail are the two-body and Dalitz decays of the light neutral mesons η, ρ, ω, η' and ϕ, which dominate dimuon production for invariant masses below ~ 1 GeV/c^2. The open charm and open beauty contributions arise from correlated semi-muonic decays of charm and beauty mesons and baryons.

The hadronic cocktail was simulated with a dedicated generator described in [25], tuned to the existing measurements whenever possible, otherwise based on the kinematic distributions extracted from PYTHIA [36]. In particular, the kinematic distributions of the ϕ-meson have been tuned by means of an iterative procedure to the results presented in this Letter to ensure self-consistency for this analysis. The open charm and beauty generation is based on a parameterisation of the spectra generated with PYTHIA [33]. The detector response for all these processes is obtained with a simulation based on the GEANT3 [37] transport code. Simulated events are then subjected to the same reconstruction and selection procedure as the data.

When describing the signal with the superposition of the aforementioned contributions, four parameters are adjusted in the fit procedure in each of the p_{T} or rapidity intervals considered in the analysis: the yield of the η, ω and ϕ-mesons, and the one of the open charm and beauty processes, with the relative beauty/charm contribution fixed (see later in this paragraph). In this way, each parameter is linked to a process dominating in at least one region of the considered mass spectrum. The remaining degrees of freedom are fixed either according to the relative branching ratios known from literature [38], or assuming specific hypotheses on the cross section ratios. In particular, the production cross section of the ρ-meson is assumed to be the same as for the ω as suggested from both models and pp data [25], while the η' contribution was derived from the η cross section by applying the ratio of the corresponding cross sections $\sigma_{\eta'}/\sigma_{\eta} = 0.3$ taken from the PYTHIA tunes ATLAS-CSC and D6T which best describe the available low-mass dimuon measurements at the LHC energies [25]. The open beauty normalisation is fixed to the open charm one via a fit of the p_{T}- and rapidity-integrated mass spectra in which the yields from both processes are free parameters; when performing differential studies, the beauty/charm ratio is scaled according to the differential distributions for the two processes, given by the Monte Carlo (MC) simulations.

For each p_{T} and rapidity interval, the raw number of ϕ-mesons is determined via a fit procedure based on a χ^2 minimisation, performed on the signal obtained after the subtraction of the combinatorial background, shown in Fig. 1 for the p_{T}-integrated samples. Several tests have been performed to evaluate the robustness of the signal extraction and estimate an appropriate systematic uncertainty for it. They include in particular:

- Replacing the fit based on the full MC hadronic cocktail with a fit based on the superposition of various empirical functions. In this case, illustrated in the right-column panels of Fig. 1, the continuum is modelled either with exponential functions or variable-width Gaussians, while the $\rho+\omega$ and ϕ peaks are described by Crystal Ball functions [39] tuned on the MC.
- Varying the ratio between the yields of open beauty and open charm processes. It was verified that for perturbations as large as $\pm 50\%$ (resulting in a reasonably wide range of variation for the shape of the total continuum) no significant systematic effect is visible.
- Varying the ratios between the two-body and Dalitz branching ratios of the η and ω-mesons, as well as the cross section ratios $\sigma_{\rho}/\sigma_{\omega}$ and $\sigma_{\eta'}/\sigma_{\eta}$, within the uncertainties coming either from the available measurements or from the differences between the PYTHIA tunes considered in the analysis of the pp data. The branching ratio $BR_{\omega\to\mu\mu}$ was taken as the average (weighted by the corresponding uncertainties) of the available measurements of $BR_{\omega\to\mu\mu}$ and $BR_{\omega\to ee}$ [38], assuming lepton universality.
- Varying the considered fit range: in particular, the fit was performed both including and excluding the mass region from 0.4 to 0.65 GeV/c^2 where the quality of the comparison between the data and the sum of the MC sources turns out to be lower.

The total systematic uncertainty on the signal extraction was taken as the quadratic sum of the above sources. The systematic uncertainty on the combinatorial background is estimated by comparing the shape of the Like-Sign dimuon contributions coming from the event mixing procedure and from the raw data [25]. This uncertainty depends on the mass, its relative contribution being maximal in the mass window 0.5–0.8 GeV/c^2 and minimal around the ϕ-meson peak, and it is added in quadrature, for each point of the mass spectrum, to the statistical uncertainty of the signal: in this way, this source of systematics is accounted for by the χ^2 minimisation procedure, and automatically propagated when evaluating the ϕ-meson raw signal from the fit parameters. The uncertainty associated to the sum of the MC sources (red band in the left-column plots of Fig. 1) is evaluated by combining the uncertainties on the normalisation of each considered process. For the processes whose normalisation is left free in the fit, this uncertainty is the statistical one resulting from the fit procedure itself; for the rest of the processes, we also propagate the systematic uncertainty on the parameters (branching ratios or cross section ratios) which fix their normalisations to those of the free processes.

4. Results

The results of the ϕ-meson analysis are presented as follows. We first present the measurement of the production cross sections, starting with its p_{T}-dependence in pp collisions at $\sqrt{s} = 2.76$ TeV, followed by p–Pb collision results as a function of p_{T} and rapidity. Then, we show the ratio of the cross sections measured in the forward and backward regions, obtained in the common rapidity interval $2.96 < |y| < 3.53$. Finally, the measurement of the nuclear modification factor R_{pPb} as a function of p_{T} is presented, separately for the p-going and the Pb-going directions.

4.1. Production cross section in pp and p–Pb collisions

The cross section σ_{ϕ} was evaluated for each p_{T} and rapidity interval as:

$$\sigma_{\phi}(x) = \frac{N^{\mathrm{raw}}_{\phi\to\mu\mu}(x)}{[A\cdot\varepsilon](x)\cdot BR_{\phi\to\mu\mu}\cdot L_{\mathrm{int}}},$$

where x stands for any specific p_{T} or rapidity interval considered. The total systematic uncertainty on $N^{\mathrm{raw}}_{\phi\to\mu\mu}(x)$, after combining the different sources described above, ranges between 3% and 8% depending on the collision system and kinematic range. The branching ratio $BR_{\phi\to\mu\mu}$ was taken from [38] as the average (weighted by the corresponding uncertainties) of the available measurements of $BR_{\phi\to\mu\mu}$ and $BR_{\phi\to ee}$, assuming lepton universality, resulting in a final uncertainty of approximately 1%. The product of the geometrical acceptance A and the reconstruction efficiency ε has been evaluated by means of MC simulations, using the cocktail predictions for the differential input spectra. The values are obtained as the ratio between the number of dimuons at the output of the reconstruction chain — including the effect of the event selection

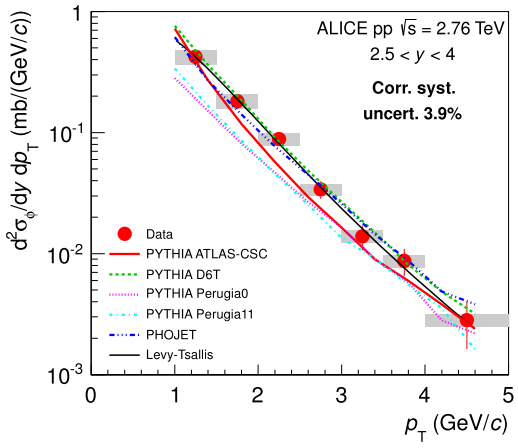


Fig. 2. ϕ-meson cross section as a function of p_{T} in pp collisions at $\sqrt{s} = 2.76$ TeV. Error bars and boxes represent statistical and systematic uncertainties, respectively. Predictions from PHOJET [42] and the PYTHIA tunes ATLAS-CSC [44], D6T [45], Perugia0 and Perugia11 [43] are also shown for comparison, as well as the result of a fit with the Levy–Tsallis function defined by Eq. (1).

criteria imposed on the data — and the number of dimuons injected as input.

The uncertainty on $[A \cdot \varepsilon]$ mainly originates from the systematic uncertainty on the dimuon tracking and trigger efficiencies. The systematic uncertainty on the tracking efficiency, amounting to 6% and 4% for the backward and forward rapidity regions, respectively, comes from the residual differences between the results of the efficiency-determination method based on reconstructed tracks [29,40], applied to both data and MC. For the systematic uncertainty on the trigger efficiency, we also refer to the procedure discussed in [29], resulting in an uncertainty of 3.2% and 2.8%, respectively, for the backward and forward rapidity regions considered in the analysis. In order to test possible additional systematic effects related to the hardware trigger p_{T} cut, imposing a non-sharp threshold around 0.5 GeV/c, the analysis was repeated with the additional offline sharp cuts $p_{\mathrm{T},\mu} > 0.5$ GeV/c and $p_{\mathrm{T},\mu} > 1$ GeV/c on single muons. For each of the two alternative scenarios, the corresponding measurement of the ϕ-meson cross section was compared to the one coming from the reference analysis: the difference between the results was found to be smaller than the quadratic difference of the statistical uncertainties, showing that no significant bias related to the trigger threshold affects the results [41].

The reported values correspond to a zero-polarisation scenario for the 2-body decay of the ϕ-meson, in the absence of evidence supporting less trivial assumptions (in particular, no measurement of ϕ-meson polarisation is currently available at the LHC energies).

4.1.1. Production cross section in pp collisions

The inclusive, p_{T}-differential ϕ-meson cross section in pp collisions at $\sqrt{s} = 2.76$ TeV is shown in Fig. 2. The data points, also summarised in Table 1, are compared with the predictions from PHOJET [42] and PYTHIA [36], where for the latter the Perugia0, Perugia11 [43], ATLAS-CSC [44], and D6T [45] tunes are considered. An overall good agreement is found between predictions and data, with the exception of the Perugia0 and Perugia11 tunes of PYTHIA which underestimate the measured cross section by a factor of two, as already observed for the ϕ-meson measurements at $\sqrt{s} = 7$ TeV [25,46]. It is worth to note that the D6T tune is not successful in describing the p_{T} evolution of the K/π ratio at mid-rapidity in pp collisions at $\sqrt{s} = 2.76$ TeV, as measured by the CMS Collaboration [47]: this suggests that hidden strangeness is better reproduced than open strangeness in this specific PYTHIA tune. Data points were fitted with a Levy–Tsallis function [48]

$$\frac{1}{p_{\mathrm{T}}}\frac{\mathrm{d}N}{\mathrm{d}p_{\mathrm{T}}} \propto \left(1 + \frac{m_{\mathrm{T}} - m_{\phi}}{nT}\right)^{-n}, \qquad (1)$$

where $m_{\mathrm{T}} = \sqrt{p_{\mathrm{T}}^2 + m_{\phi}^2}$ stands for the transverse mass, obtaining the values $n = 10.2 \pm 4.8$ and $T = 284 \pm 72$ MeV for the fit parameters, where the errors reflect the statistical uncertainties only. The cross section integrated over the accessible p_{T} range $1 < p_{\mathrm{T}} < 5$ GeV/c is $\sigma_{\phi} = 0.566 \pm 0.055$ (stat.) ± 0.044 (syst.) mb. The systematic uncertainties for this measurement are summarised in Table 2.

Table 1
p_{T}-differential production cross section for the ϕ-meson in pp collisions at $\sqrt{s} = 2.76$ TeV, for $2.5 < y < 4$. The first uncertainty is statistical and the second is the bin-to-bin uncorrelated systematic. The bin-to-bin correlated relative systematic uncertainty is 3.9%. The χ^2/ndf values are relative to the hadronic-cocktail fit and the [0.8, 1.2 GeV/c^2] mass region, where ndf = 10.

p_{T} (GeV/c)	χ^2/ndf	$\mathrm{d}^2\sigma_{\phi}/(\mathrm{d}y\mathrm{d}p_{\mathrm{T}})$ (mb/(GeV/c))
[1.0, 1.5]	1.1	$0.423 \pm 0.067 \pm 0.043$
[1.5, 2.0]	1.7	$0.182 \pm 0.025 \pm 0.018$
[2.0, 2.5]	1.1	$0.089 \pm 0.011 \pm 0.007$
[2.5, 3.0]	1.1	$0.0340 \pm 0.0056 \pm 0.0020$
[3.0, 3.5]	0.9	$0.0139 \pm 0.0032 \pm 0.0011$
[3.5, 4.0]	1.1	$0.0087 \pm 0.0022 \pm 0.0006$
[4.0, 5.0]	1.1	$0.0028 \pm 0.0012 \pm 0.0002$

Table 2
Systematic uncertainties (in percent) contributing to the measurement of the ϕ cross section in pp collisions at $\sqrt{s} = 2.76$ TeV. When the uncertainty values depend on the p_{T} interval, their minimum and maximum values are quoted.

Source	Syst. uncertainty on $\sigma_{\phi}^{\mathrm{pp}}$
Uncorrelated	
Signal extraction	3–8%
Tracking efficiency	4%
Trigger efficiency	3%
Correlated	
L_{int}	3.8%
$BR(\phi \to \ell\ell)$	1%

4.1.2. Production cross section in p–Pb collisions

The ϕ cross section as a function of p_{T} in p–Pb collisions is shown in Fig. 3 for the forward and backward rapidity regions considered in the analysis. The results, also reported in Table 3, are fitted with the Levy–Tsallis distribution defined in Eq. (1), the resulting fit parameters being $\beta = 9.6 \pm 1.3$ and $T = 366 \pm 30$ MeV for the forward rapidity region and $\beta = 11.4 \pm 1.4$ and $T = 384 \pm 24$ MeV for the backward one, where the errors reflect the statistical uncertainties only. The predictions from HIJING (with gluon shadowing) [49] and DPMJET [50] are also shown: these generators provided a good description of the ALICE $\mathrm{d}N_{\mathrm{ch}}/\mathrm{d}\eta_{\mathrm{lab}}$ results at mid-rapidity [9]. Averaging over the available p_{T} range, the discrepancy between the data and the predictions from HIJING and DPMJET amounts to $\sim 18\%$ and $\sim 57\%$, respectively, at backward rapidity (the Pb-going direction) and $\sim 5\%$ and $\sim 9.5\%$, respectively, at forward rapidity (the p-going direction). In all the cases, the generators underestimate the data points.

The ϕ cross section in p–Pb collisions, integrated over the accessible p_{T} range, $1 < p_{\mathrm{T}} < 7$ GeV/c, is shown as a function of rapidity in Fig. 4. The data points, also summarised in Table 4, exhibit a significant asymmetry between the forward and backward rapidity regions. The data point from the ϕ-meson analysis at mid-rapidity in the $\mathrm{K}^+\mathrm{K}^-$ channel [51], also shown for the

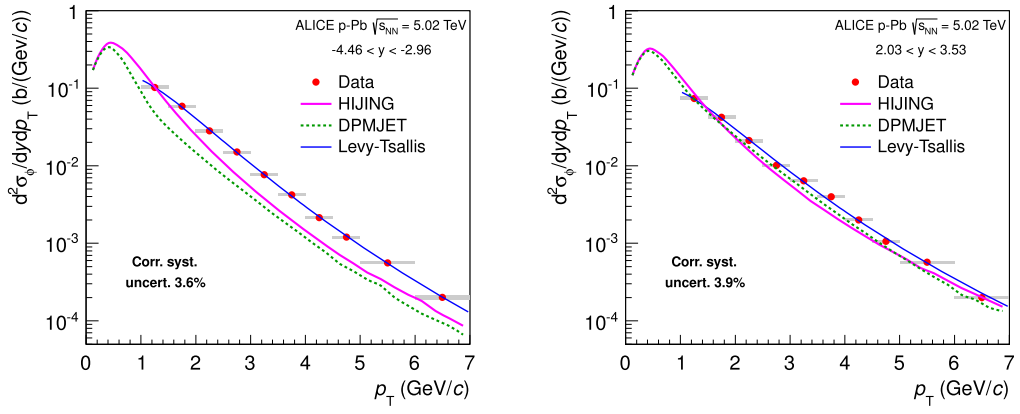


Fig. 3. ϕ-meson cross section in p–Pb collisions at $\sqrt{s_{NN}} = 5.02$ TeV as a function of p_T in the backward (left) and forward (right) rapidity regions. Error bars (smaller than the markers) and boxes represent statistical and systematic uncertainties, respectively. Predictions by HIJING [49] and DPMJET [50] are also shown, together with the result of a fit with the Levy–Tsallis function (Eq. (1)).

Table 3
Production cross section for the ϕ-meson in p–Pb collisions at $\sqrt{s_{NN}} = 5.02$ TeV, as a function of p_T, in the backward and forward rapidity regions. The first uncertainty is statistical and the second is the bin-to-bin uncorrelated systematic. The bin-to-bin correlated relative systematic uncertainty is 3.6% and 3.9%, respectively, for the backward and the forward regions. The χ^2/ndf values are relative to the hadronic-cocktail fit and the [0.8, 1.2 GeV/c^2] mass region.

p_T (GeV/c)	$-4.46 < y < -2.96$		$2.03 < y < 3.53$	
	χ^2/ndf	$d^2\sigma_\phi^{pPb}/(dydp_T)$ (mb/(GeV/c))	χ^2/ndf	$d^2\sigma_\phi^{pPb}/(dydp_T)$ (mb/(GeV/c))
[1.0, 1.5]	0.7	$102 \pm 8 \pm 12$	1.5	$73.3 \pm 5.6 \pm 8.0$
[1.5, 2.0]	1.2	$58.6 \pm 3.3 \pm 5.5$	1.9	$42.1 \pm 2.5 \pm 4.3$
[2.0, 2.5]	2.5	$28.3 \pm 1.4 \pm 2.9$	1.7	$21.0 \pm 1.2 \pm 2.0$
[2.5, 3.0]	4.2	$15.0 \pm 0.7 \pm 1.2$	3.1	$10.07 \pm 0.77 \pm 0.97$
[3.0, 3.5]	2.6	$7.66 \pm 0.40 \pm 0.70$	2.0	$6.38 \pm 0.41 \pm 0.61$
[3.5, 4.0]	1.9	$4.20 \pm 0.24 \pm 0.34$	1.2	$3.96 \pm 0.30 \pm 0.36$
[4.0, 4.5]	0.7	$2.15 \pm 0.17 \pm 0.16$	1.0	$1.99 \pm 0.20 \pm 0.15$
[4.5, 5.0]	0.9	$1.20 \pm 0.11 \pm 0.10$	0.9	$1.06 \pm 0.13 \pm 0.08$
[5.0, 6.0]	1.0	$0.560 \pm 0.052 \pm 0.054$	1.0	$0.570 \pm 0.088 \pm 0.043$
[6.0, 7.0]	1.2	$0.201 \pm 0.030 \pm 0.028$	0.9	$0.199 \pm 0.045 \pm 0.016$

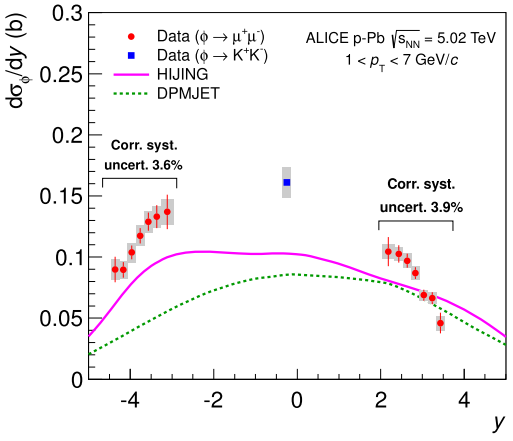


Fig. 4. ϕ cross section in p–Pb collisions at $\sqrt{s_{NN}} = 5.02$ TeV as a function of rapidity, integrated over the range $1 < p_T < 7$ GeV/c. Error bars and boxes represent statistical and systematic uncertainties, respectively. Predictions by HIJING and DPMJET are also shown, together with the mid-rapidity data point from the ϕ-meson measurement in the K^+K^- channel [51], also evaluated in the range $1 < p_T < 7$ GeV/c.

$1 < p_T < 7$ GeV/c p_T range, fits well into the trend defined by the two series of points in the backward and forward rapidity regions. This observation complements the previous measurements of light-flavour particle production (charged unidentified particles) reported in p–Pb by ALICE at the LHC at mid-rapidity [9], and in d–Au by PHOBOS at RHIC ranging from mid to forward rapidity [14]. The comparison between the data and the predictions by

Table 4
Production cross section for the ϕ-meson in p–Pb collisions at $\sqrt{s_{NN}} = 5.02$ TeV, as a function of rapidity, integrated over the range $1 < p_T < 7$ GeV/c. The first uncertainty is statistical and the second is the bin-to-bin uncorrelated systematic. The bin-to-bin correlated relative systematic uncertainty is 3.6% and 3.9%, respectively, for the backward and the forward regions. The χ^2/ndf values are relative to the hadronic-cocktail fit and the [0.8, 1.2 GeV/c^2] mass region.

y	χ^2/ndf	$d\sigma_\phi^{pPb}/dy$ (mb)	y	χ^2/ndf	$d\sigma_\phi^{pPb}/dy$ (mb)
[−4.46, −4.25]	0.9	$89 \pm 10 \pm 9$	[2.03, 2.35]	2.6	$104 \pm 11 \pm 6$
[−4.25, −4.05]	1.8	$89 \pm 6 \pm 7$	[2.35, 2.55]	1.5	$102 \pm 7 \pm 5$
[−4.05, −3.85]	0.9	$103 \pm 5 \pm 8$	[2.55, 2.75]	2.0	$96 \pm 5 \pm 6$
[−3.85, −3.65]	2.9	$117 \pm 6 \pm 9$	[2.75, 2.95]	1.6	$86 \pm 4 \pm 5$
[−3.65, −3.45]	1.2	$128 \pm 7 \pm 9$	[2.95, 3.15]	2.3	$68 \pm 4 \pm 4$
[−3.45, −3.25]	3.6	$133 \pm 9 \pm 9$	[3.15, 3.35]	1.0	$66 \pm 5 \pm 5$
[−3.25, −2.96]	1.2	$136 \pm 14 \pm 11$	[3.35, 3.53]	1.2	$45 \pm 8 \pm 6$

HIJING and DPMJET, illustrated in Fig. 4, clearly shows how the models — which successfully described charged particle production at mid-rapidity in the same collision system [9] — fail to properly reproduce the shape and the normalisation of the observed rapidity dependence of the ϕ cross section. Still, the HIJING prediction qualitatively reproduces the forward–backward asymmetry observed in the data, as well as — ignoring the normalisation — the shape of the y-dependence in the backward region. DPMJET, on the contrary, fails to reproduce even qualitatively the observed forward–backward asymmetry.

4.2. Forward–backward ratio in p–Pb collisions

To establish a more direct comparison of the cross section in the p-going and Pb-going directions, σ_ϕ^{pPb} was extracted as a func-

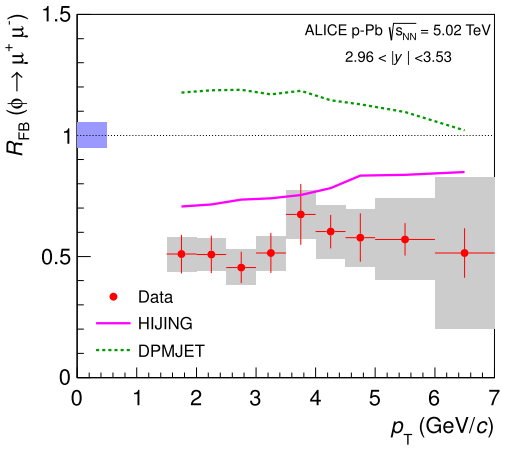


Fig. 5. Forward–backward ratio for the ϕ-meson in p–Pb collisions at $\sqrt{s_{NN}} = 5.02$ TeV as a function of p_T, in the rapidity range $2.96 < |y| < 3.53$ common to the two rapidity regions considered in the analysis. Error bars and boxes represent statistical and systematic uncertainties, respectively. The blue box on the left represents the bin-to-bin correlated systematic uncertainty, see Table 7. Predictions from HIJING and DPMJET are also shown for comparison. (For interpretation of the references to colour in this figure legend, the reader is referred to the web version of this article.)

tion of p_T in the common $|y|$ range $2.96 < |y| < 3.53$. The p_T interval $1.0 < p_T < 1.5$ GeV/c was discarded in this measurement because of the poor statistics available in this limited rapidity range, resulting in an uncertainty larger than 50%.

The ratio between the forward and backward cross section, R_{FB}, is shown as a function of p_T in Fig. 5. The data points exhibit no significant p_T dependence within the experimental uncertainties. Predictions by HIJING and DPMJET are also shown, with HIJING slightly overestimating the data points and DPMJET clearly failing to reproduce the observed values, staying above $R_{FB} = 1$ in the whole p_T range considered here. This observation is consistent with the observations in Fig. 4, where the forward–backward asymmetry of the ϕ-meson yield was better reproduced by HIJING than by DPMJET.

4.3. Nuclear modification factor in p–Pb collisions

The ϕ-meson nuclear modification factor R_{pPb} is defined as the ratio between the production cross section $\sigma_\phi^{pPb}(p_T)$ in p–Pb collisions and the cross section $\sigma_\phi^{pp}(p_T)$ in pp collisions — evaluated at $\sqrt{s} = 5.02$ TeV as described in the following — scaled by A_{Pb}:

$$R_{pPb}(p_T) = \frac{\sigma_\phi^{pPb}(p_T)}{\sigma_\phi^{pp}(p_T) \cdot A_{Pb}}\,, \qquad (2)$$

where A_{Pb} is the nuclear mass number for the Pb nucleus. Since for the pp cross section σ_ϕ^{pp} at $\sqrt{s} = 5.02$ TeV no direct measurement is currently available, it was evaluated by interpolating the measurements in the rapidity interval $2.5 < y < 4$ at $\sqrt{s} = 2.76$ (see Section 4.1.1) and 7 TeV [25]. For each p_T interval, the $\sqrt{s}$ dependence of the differential cross section $d^2\sigma_\phi^{pp}/(dy\,dp_T)$ was described with a power law $\sigma^{pp}(\sqrt{s}) = C \cdot (\sqrt{s})^\alpha$, where C and α are determined using the data at 2.76 and 7 TeV. Alternative parameterisations were also considered [52], namely a linear and an exponential function, and the mean of the results obtained with the three functions was taken. Since the pp measurements are limited to $1 < p_T < 5$ GeV/c, the cross section at $\sqrt{s_{NN}} = 5.02$ TeV was extrapolated towards higher p_T by means of a Levy–Tsallis function, which describes the calculated differential cross section in the p_T range covered by the measurements. The uncertainty

Table 5
Differential cross section for the ϕ-meson in pp collisions at $\sqrt{s} = 5.02$ TeV in the backward and forward rapidity regions of interest for the analysis of the p–Pb data, as obtained interpolating the available measurements at $\sqrt{s} = 2.76$ and 7 TeV. Total uncertainties, combining statistical and systematic sources, are reported.

p_T (GeV/c)	$d^2\sigma_\phi/dydp_T$ (mb/(GeV/c))	
	$-4.46 < y < -2.96$	$2.03 < y < 3.53$
[1.0, 1.5]	0.491 ± 0.067	0.656 ± 0.090
[1.5, 2.0]	0.223 ± 0.015	0.297 ± 0.020
[2.0, 2.5]	0.0995 ± 0.0071	0.1328 ± 0.0095
[2.5, 3.0]	0.0467 ± 0.0032	0.0623 ± 0.0043
[3.0, 3.5]	0.0234 ± 0.0015	0.0312 ± 0.0020
[3.5, 4.0]	0.0125 ± 0.0011	0.0167 ± 0.0015
[4.0, 4.5]	0.00706 ± 0.00094	0.0094 ± 0.0012
[4.5, 5.0]	0.00419 ± 0.00082	0.0056 ± 0.0011
[5.0, 6.0]	0.00213 ± 0.00060	0.00284 ± 0.00081
[6.0, 7.0]	0.00093 ± 0.00039	0.00124 ± 0.00052

on the interpolated cross sections arises from the choice of the function used for the interpolation, from the uncertainties in the measurements at 2.76 and 7 TeV, and — for $p_T > 5$ GeV/c — from the extrapolation based on the Levy–Tsallis fit. They range from about 7% for $p_T = 1$ GeV/c to 20% for $p_T = 5$ GeV/c, and exceed 30% for $p_T > 5$ GeV/c, representing the major source of systematic uncertainty for the measurement of the nuclear modification factor. The interpolated cross section, which refers to the rapidity range $2.5 < y < 4$, was finally scaled to the forward and backward rapidity windows $2.03 < y < 3.53$ and $-4.46 < y < -2.96$, considered for the analysis of the p–Pb data. The relative scaling factors $f_{fwd} = 1.135 \pm 0.031$ and $f_{bkw} = 0.850 \pm 0.028$ were evaluated as an average from simulations with PHOJET and the Perugia0, Perugia11, ATLAS-CSC and D6T PYTHIA tunes. In doing so, we also retained the PYTHIA tunes which were observed to fail in describing the pp data (see Section 4.1.1): the reason is that the disagreement between models and data concerns in this case the absolute normalisation more than the shape of the kinematic distributions, which is the only relevant feature in the evaluation of the f_{fwd} and f_{bkw} factors. The uncertainties (amounting to about 3%) correspond to the differences between the considered MC predictions. The numerical values are reported in Table 5.

The nuclear modification factor R_{pPb} as a function of p_T is shown in the two panels of Fig. 6 for the backward and forward rapidity regions considered in the analysis. The numerical values are also quoted in Table 6. For each p_T interval, the systematic uncertainty detailed in Table 7 results from the quadratic sum of the uncertainty on the ϕ cross section in p–Pb and the one of the pp reference. A rising trend of R_{pPb} when going from $p_T = 1$ GeV/c to $p_T \approx 3$–4 GeV/c can be observed both at backward and forward rapidity. The values of R_{pPb} in the two rapidity ranges, however, are significantly different. In particular, at backward rapidity we observe an enhancement of the ϕ cross section with respect to the scaled pp reference peaked around $p_T = 3$–4 GeV/c. This enhancement, absent in the forward rapidity region, reaches a factor of up to ~ 1.6 and could be associated either to an initial-state effect (including a possible Cronin-like enhancement [4,53]) or to a final state effect related to radial flow in p–Pb as proposed for recent ALICE measurements at mid-rapidity [12]. Discriminating between these two effects requires more detailed investigations, including differential analyses as a function of global event properties like collision centrality.

Concerning the behaviour at high p_T, we observe that the ϕ-meson R_{pPb} is compatible with unity for $p_T \gtrsim 4$ GeV/c in the p-going direction, similar to what was observed for the R_{pPb} of charged particle production at mid-rapidity [10,12]. The observations in the Pb-going direction do not allow a clear trend of the R_{pPb} factor at high p_T to be established. A possible saturation at

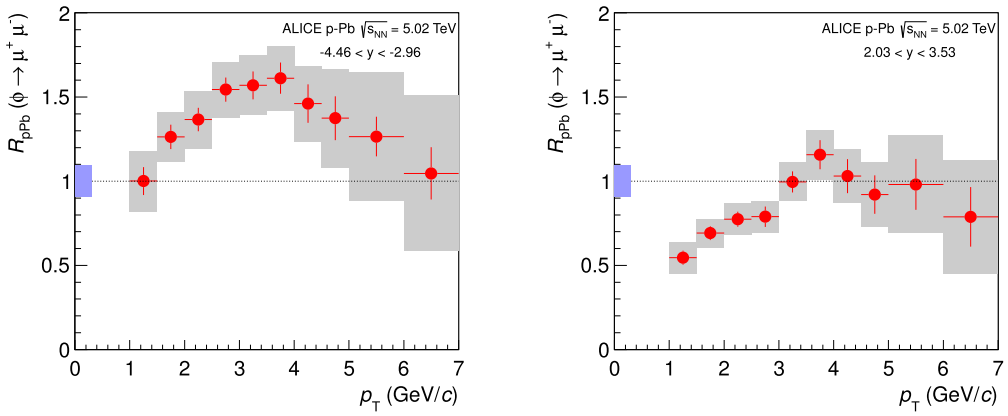


Fig. 6. Nuclear modification factor $R_{\rm pPb}$ in p–Pb collisions at $\sqrt{s_{\rm NN}} = 5.02$ TeV for the ϕ-meson as a function of $p_{\rm T}$, in the backward (left) and forward (right) rapidity regions considered in the analysis. Error bars and boxes represent statistical and bin-to-bin uncorrelated systematic uncertainties, respectively. The blue box on the left represents the bin-to-bin correlated systematic uncertainty, see Table 7. (For interpretation of the references to colour in this figure legend, the reader is referred to the web version of this article.)

Table 6
Nuclear modification factor $R_{\rm pPb}$ in p–Pb collisions at $\sqrt{s_{\rm NN}} = 5.02$ TeV for the ϕ-meson as a function of $p_{\rm T}$ in the backward and forward rapidity regions. The first uncertainty is statistical and the second is the bin-to-bin uncorrelated systematic. The bin-to-bin correlated relative systematic uncertainty is 8%.

$p_{\rm T}$ (GeV/c)	$R_{\rm pPb}$	
	$-4.46 < y < -2.96$	$2.03 < y < 3.53$
[1.0, 1.5]	$1.00 \pm 0.08 \pm 0.18$	$0.537 \pm 0.041 \pm 0.094$
[1.5, 2.0]	$1.26 \pm 0.07 \pm 0.15$	$0.681 \pm 0.040 \pm 0.083$
[2.0, 2.5]	$1.37 \pm 0.07 \pm 0.17$	$0.760 \pm 0.043 \pm 0.091$
[2.5, 3.0]	$1.54 \pm 0.07 \pm 0.16$	$0.777 \pm 0.059 \pm 0.092$
[3.0, 3.5]	$1.57 \pm 0.08 \pm 0.18$	$0.98 \pm 0.06 \pm 0.11$
[3.5, 4.0]	$1.62 \pm 0.09 \pm 0.19$	$1.14 \pm 0.09 \pm 0.15$
[4.0, 4.5]	$1.46 \pm 0.12 \pm 0.22$	$1.02 \pm 0.10 \pm 0.15$
[4.5, 5.0]	$1.38 \pm 0.13 \pm 0.29$	$0.91 \pm 0.11 \pm 0.19$
[5.0, 6.0]	$1.26 \pm 0.12 \pm 0.38$	$0.97 \pm 0.15 \pm 0.29$
[6.0, 7.0]	$1.04 \pm 0.16 \pm 0.46$	$0.77 \pm 0.17 \pm 0.33$

Table 7
Systematic uncertainties (in percent) contributing to the measurement of the ϕ cross section and nuclear modification factor in the backward and forward rapidity regions in p–Pb collisions at $\sqrt{s_{\rm NN}} = 5.02$ TeV. When the uncertainty values depend on the $p_{\rm T}$ interval, their minimum and maximum values are quoted.

Source	Syst. uncertainty on $\sigma_\phi^{\rm pPb}$ and $R_{\rm pPb}$	
	$-4.46 < y < -2.96$	$2.03 < y < 3.53$
Uncorrelated		
Signal extraction	3–5%	4–8%
Tracking efficiency	6%	4%
Trigger efficiency	3.2%	2.8%
$\sigma_\phi^{\rm pp}$	7–30%	7–30%
Correlated		
$L_{\rm int}$	3.5%	3.8%
$BR(\phi \to \ell\ell)$	1%	1%
$f_{\rm bkw}$	3.3%	–
$f_{\rm fwd}$	–	2.7%

$R_{\rm pPb} \approx 1$ for $p_{\rm T} \gtrsim 5$ GeV/c is, however, still compatible with the measurements.

Only few other existing measurements can be compared to our data. In particular, results on ϕ-meson production in d–Au collisions at $\sqrt{s_{\rm NN}} = 200$ GeV have been recently released by the PHENIX Collaboration [54]. The $p_{\rm T}$-dependence of the $R_{\rm dAu}$ measured by PHENIX, as well as its evolution from backward to forward rapidity, is found to be similar to what is observed in our results for $R_{\rm pPb}$. Mid-rapidity data on $R_{\rm dAu}$, also presented by the PHENIX Collaboration for the ϕ-meson, seem to sit between the forward- and backward-rapidity results. Forward-rapidity measurements in d–Au collisions at $\sqrt{s_{\rm NN}} = 200$ GeV at RHIC [13,14] are also available for unidentified charged particles, although for the d-going direction only. These data exhibit, similar to our ϕ-meson results in the p-going direction, a rise of $R_{\rm dAu}$ from ~ 0.5 to ~ 1 between $p_{\rm T} \sim 1$ GeV/c and $p_{\rm T} \sim 4$ GeV/c. A similar rise of $R_{\rm pPb}$ in p–Pb collisions at $\sqrt{s_{\rm NN}} = 5.02$ TeV is also observed in the already cited measurement of unidentified charged particle and identified charged pion and kaon production at mid-rapidity performed by ALICE [10,12]. A recent study of ϕ-meson production in p–Pb collisions at mid-rapidity by ALICE [51] does not currently include results on $R_{\rm pPb}$.

5. Conclusions

We have presented results on ϕ-meson production in the dimuon channel in p–Pb collisions at $\sqrt{s_{\rm NN}} = 5.02$ TeV obtained by the ALICE experiment at the LHC. Cross section and nuclear modification factor measurements were performed for $1 < p_{\rm T} < 7$ GeV/c in the rapidity windows $2.03 < y < 3.53$ (p-going direction) and $-4.46 < y < -2.96$ (Pb-going direction). A corresponding cross section measurement in pp collisions at $\sqrt{s} = 2.76$ TeV has also been reported, for $1 < p_{\rm T} < 5$ GeV/c in the region $2.5 < y < 4$. Predictions from HIJING and DPMJET are compared to the p–Pb cross sections and are found to underestimate the data both at backward (by about 18% and 57% on average, respectively) and at forward rapidity (by about 5% and 9.5% on average, respectively). The forward–backward ratio in the ϕ-meson cross section in p–Pb collisions was measured in the rapidity range $2.96 < |y| < 3.53$, and no significant $p_{\rm T}$ dependence was found within uncertainties. In this case, the data points are significantly overestimated by the DPMJET model, while only a slight disagreement is observed with respect to the HIJING prediction.

In the p-going direction a rising trend of the nuclear modification factor $R_{\rm pPb}$ is observed from ~ 0.5 to ~ 1, when going from $p_{\rm T} = 1$ GeV/c to $p_{\rm T} = 4$ GeV/c. This observation is compatible with the behaviour of charged particles at forward rapidity at RHIC energies, and at mid-rapidity at LHC energies. In the Pb-going direction, on the other hand, an enhancement is observed for $R_{\rm pPb}$, reaching values as large as ~ 1.6 around $p_{\rm T} = 3$–4 GeV/c. An interpretation of these results, either in terms of an initial-state (Cronin-like) effect or a final-state effect related to radial flow in p–Pb, is not possible yet, due to a general lack of theoretical predictions for particle production in the light-flavour sector at forward rapidity in p–A collisions at the LHC energies.

Acknowledgements

The ALICE Collaboration would like to thank all its engineers and technicians for their invaluable contributions to the construction of the experiment and the CERN accelerator teams for the outstanding performance of the LHC complex. The ALICE Collaboration gratefully acknowledges the resources and support provided by all Grid centres and the Worldwide LHC Computing Grid (WLCG) Collaboration. The ALICE Collaboration acknowledges the following funding agencies for their support in building and running the ALICE detector: A. I. Alikhanyan National Science Laboratory (Yerevan Physics Institute) Foundation (ANSL), State Committee of Science and World Federation of Scientists (WFS), Armenia; Austrian Academy of Sciences and Nationalstiftung für Forschung, Technologie und Entwicklung, Austria; Conselho Nacional de Desenvolvimento Científico e Tecnológico (CNPq), Universidade Federal do Rio Grande do Sul (UFRGS), Financiadora de Estudos e Projetos (Finep) and Fundação de Amparo à Pesquisa do Estado de São Paulo (FAPESP), Brazil; Ministry of Science and Technology of the People's Republic of China (MOST), National Natural Science Foundation of China (NSFC) and Ministry of Education of China (MOE), China; Ministry of Science, Education and Sports and Croatian Science Foundation, Croatia; Ministry of Education, Youth and Sports of the Czech Republic, Czech Republic; The Danish Council for Independent Research – Natural Sciences, the Carlsberg Foundation and Danish National Research Foundation (DNRF), Denmark; Helsinki Institute of Physics (HIP), Finland; Commissariat à l'Energie Atomique (CEA) and Institut National de Physique Nucléaire et de Physique des Particules (IN2P3) and Centre National de la Recherche Scientifique (CNRS), France; Bundesministerium für Bildung, Wissenschaft, Forschung und Technologie (BMBF) and GSI Helmholtzzentrum für Schwerionenforschung GmbH, Germany; Ministry of Education, Research and Religious Affairs, Greece; National Research, Development and Innovation Office, Hungary; Department of Atomic Energy, Government of India (DAE) and Council of Scientific and Industrial Research (CSIR), New Delhi, India; Indonesian Institute of Science, Indonesia; Centro Fermi – Museo Storico della Fisica e Centro Studi e Ricerche Enrico Fermi and Instituto Nazionale di Fisica Nucleare (INFN), Italy; Institute for Innovative Science and Technology, Nagasaki Institute of Applied Science (IIST), Japan Society for the Promotion of Science (JSPS) KAKENHI and Japanese Ministry of Education, Culture, Sports, Science, and Technology (MEXT), Japan; Consejo Nacional de Ciencia (CONACYT) y Tecnología, through Fondo de Cooperación Internacional en Ciencia y Tecnología (FONCICYT) and Dirección General de Asuntos del Personal Academico (DGAPA), Mexico; Nationaal instituut voor subatomaire fysica (Nikhef), Netherlands; The Research Council of Norway, Norway; Commission on Science and Technology for Sustainable Development in the South (COMSATS), Pakistan; Pontificia Universidad Católica del Perú, Peru; Ministry of Science and Higher Education and National Science Centre, Poland; Korea Institute of Science and Technology Information and National Research Foundation of Korea (NRF), Republic of Korea; Ministry of Education and Scientific Research, Institute of Atomic Physics and Romanian National Agency for Science, Technology and Innovation, Romania; Joint Institute for Nuclear Research (JINR), Ministry of Education and Science of the Russian Federation and National Research Centre Kurchatov Institute, Russia; Ministry of Education, Science, Research and Sport of the Slovak Republic, Slovakia; National Research Foundation of South Africa, South Africa; Centro de Aplicaciones Tecnológicas y Desarrollo Nuclear (CEADEN), Cubaenergía, Cuba, Ministerio de Ciencia e Innovación and Centro de Investigaciones Energéticas, Medioambientales y Tecnológicas (CIEMAT), Spain; Swedish Research Council (VR) and Knut and Alice Wallenberg Foundation (KAW), Sweden; European Organization for Nuclear Research, Switzerland; National Science and Technology Development Agency (NSDTA), Suranaree University of Technology (SUT) and Office of the Higher Education Commission under NRU project of Thailand, Thailand; Turkish Atomic Energy Agency (TAEK), Turkey; National Academy of Sciences of Ukraine, Ukraine; Science and Technology Facilities Council (STFC), United Kingdom; National Science Foundation of the United States of America (NSF) and United States Department of Energy, Office of Nuclear Physics (DOE NP), United States of America.

References

[1] A. Bazavov, T. Bhattacharya, M. Cheng, C. DeTar, H. Ding, et al., The chiral and deconfinement aspects of the QCD transition, Phys. Rev. D 85 (2012) 054503, arXiv:1111.1710 [hep-lat].

[2] Wuppertal–Budapest Collaboration, S. Borsanyi, et al., Is there still any T_c mystery in lattice QCD? Results with physical masses in the continuum limit III, J. High Energy Phys. 1009 (2010) 073, arXiv:1005.3508 [hep-lat].

[3] S. Borsanyi, G. Endrodi, Z. Fodor, A. Jakovac, S.D. Katz, et al., The QCD equation of state with dynamical quarks, J. High Energy Phys. 1011 (2010) 077, arXiv:1007.2580 [hep-lat].

[4] A. Accardi, Cronin effect in proton nucleus collisions: a survey of theoretical models, arXiv:hep-ph/0212148.

[5] C. Salgado, J. Alvarez-Muniz, F. Arleo, N. Armesto, M. Botje, et al., Proton–nucleus collisions at the LHC: scientific opportunities and requirements, J. Phys. G 39 (2012) 015010, arXiv:1105.3919 [hep-ph].

[6] M. Brandt, M. Klasen, F. König, Nuclear parton density modifications from low-mass lepton pair production at the LHC, Nucl. Phys. A 927 (2014) 78–90, arXiv:1401.6817 [hep-ph].

[7] BRAHMS Collaboration, I. Arsene, et al., Quark gluon plasma and color glass condensate at RHIC? The perspective from the BRAHMS experiment, Nucl. Phys. A 757 (2005) 1–27, arXiv:nucl-ex/0410020.

[8] B. Back, M. Baker, M. Ballintijn, D. Barton, B. Becker, et al., The PHOBOS perspective on discoveries at RHIC, Nucl. Phys. A 757 (2005) 28–101, arXiv:nucl-ex/0410022.

[9] ALICE Collaboration, B. Abelev, et al., Pseudorapidity density of charged particles p–Pb collisions at $\sqrt{s_{NN}} = 5.02$ TeV, Phys. Rev. Lett. 110 (2013) 032301, arXiv:1210.3615 [nucl-ex].

[10] ALICE Collaboration, B. Abelev, et al., Transverse momentum distribution and nuclear modification factor of charged particles in p–Pb collisions at $\sqrt{s_{NN}} = 5.02$ TeV, Phys. Rev. Lett. 110 (2013) 082302, arXiv:1210.4520 [nucl-ex].

[11] ALICE Collaboration, B. Abelev, et al., Transverse momentum dependence of inclusive primary charged-particle production in p–Pb collisions at $\sqrt{s_{NN}} = 5.02$ TeV, Eur. Phys. J. C 74 (9) (2014) 3054, arXiv:1405.2737 [nucl-ex].

[12] ALICE Collaboration, J. Adam, et al., Multiplicity dependence of charged pion, kaon, and (anti)proton production at large transverse momentum in p–Pb collisions at $\sqrt{s_{NN}} = 5.02$ TeV, Phys. Lett. B 760 (2016) 720–735, arXiv:1601.03658 [nucl-ex].

[13] BRAHMS Collaboration, I. Arsene, et al., On the evolution of the nuclear modification factors with rapidity and centrality in d+Au collisions at $\sqrt{s_{NN}} = 200$ GeV, Phys. Rev. Lett. 93 (2004) 242303, arXiv:nucl-ex/0403005.

[14] PHOBOS Collaboration, B. Back, et al., Pseudorapidity distribution of charged particles in d+Au collisions at $\sqrt{s_{NN}} = 200$ GeV, Phys. Rev. Lett. 93 (2004) 082301, arXiv:nucl-ex/0311009.

[15] J. Rafelski, B. Muller, Strangeness production in the quark–gluon plasma, Phys. Rev. Lett. 48 (1982) 1066.

[16] A. Shor, ϕ-Meson production as a probe of the quark gluon plasma, Phys. Rev. Lett. 54 (1985) 1122–1125.

[17] P. Koch, B. Muller, J. Rafelski, Strangeness in relativistic heavy ion collisions, Phys. Rep. 142 (1986) 167–262.

[18] NA49 Collaboration, C. Alt, et al., System-size dependence of strangeness production in nucleus–nucleus collisions at $\sqrt{s_{NN}} = 17.3$ GeV, Phys. Rev. Lett. 94 (2005) 052301, arXiv:nucl-ex/0406031.

[19] NA49 Collaboration, C. Alt, et al., Energy dependence of ϕ meson production in central Pb+Pb collisions at $\sqrt{s_{NN}} = 6$ to 17 GeV, Phys. Rev. C 78 (2008) 044907, arXiv:0806.1937 [nucl-ex].

[20] NA50 Collaboration, B. Alessandro, et al., ϕ production in Pb–Pb collisions at 158-GeV/c per nucleon incident momentum, Phys. Lett. B 555 (2003) 147–155; NA50 Collaboration, B. Alessandro, et al., Phys. Lett. B 561 (2003) 294 (Erratum).

[21] NA60 Collaboration, K. Banicz, et al., ϕ production in In–In collisions at 158-A-GeV, Eur. Phys. J. C 64 (2009) 1–18, arXiv:0906.1102 [hep-ex].

[22] NA60 Collaboration, R. Arnaldi, et al., A comparative measurement of $\phi \to K^+K^-$ and $\phi \to \mu^+\mu^-$ in In–In collisions at the CERN SPS, Phys. Lett. B 699 (2011) 325–329, arXiv:1104.4060 [nucl-ex].

[23] STAR Collaboration, B. Abelev, et al., Measurements of ϕ meson production in relativistic heavy-ion collisions at RHIC, Phys. Rev. C 79 (2009) 064903, arXiv:0809.4737 [nucl-ex].
[24] PHENIX Collaboration, S.S. Adler, et al., Production of ϕ mesons at mid-rapidity in $\sqrt{s_{NN}} = 200$ GeV Au+Au collisions at RHIC, Phys. Rev. C 72 (2005) 014903, arXiv:nucl-ex/0410012.
[25] ALICE Collaboration, B. Abelev, et al., Light vector meson production in pp collisions at $\sqrt{s} = 7$ TeV, Phys. Lett. B 710 (2012) 557–568, arXiv:1112.2222 [nucl-ex].
[26] ALICE Collaboration, K. Aamodt, et al., The ALICE experiment at the CERN LHC, J. Instrum. 3 (2008) S08002.
[27] ALICE Collaboration, B. Abelev, et al., Performance of the ALICE experiment at the CERN LHC, Int. J. Mod. Phys. A 29 (2014) 1430044, arXiv:1402.4476 [nucl-ex].
[28] ALICE Collaboration, M. Gagliardi, Measurement of reference cross sections in pp and Pb–Pb collisions at the LHC in van der Meer scans with the ALICE detector, AIP Conf. Proc. 1422 (2012) 110–116, arXiv:1109.5369 [hep-ex].
[29] ALICE Collaboration, B. Abelev, et al., J/ψ production and nuclear effects in p–Pb collisions at $\sqrt{s_{NN}} = 5.02$ TeV, J. High Energy Phys. 1402 (2014) 073, arXiv:1308.6726 [nucl-ex].
[30] ALICE Collaboration, B. Abelev, et al., Measurement of visible cross sections in proton–lead collisions at $\sqrt{s_{NN}} = 5.02$ TeV in van der Meer scans with the ALICE detector, J. Instrum. 9 (11) (2014) P11003, arXiv:1405.1849 [nucl-ex].
[31] ALICE Collaboration, B. Abelev, et al., Measurement of quarkonium production at forward rapidity in pp collisions at $\sqrt{s} = 7$ TeV, Eur. Phys. J. C 74 (8) (2014) 2974, arXiv:1403.3648 [nucl-ex].
[32] ALICE Collaboration, B. Abelev, et al., Measurement of inelastic, single- and double-diffraction cross sections in proton–proton collisions at the LHC with ALICE, Eur. Phys. J. C 73 (6) (2013) 2456, arXiv:1208.4968 [hep-ex].
[33] ALICE Collaboration, L. Aphecetche, et al., Numerical Simulations and Offline Reconstruction of the Muon Spectrometer of ALICE, 2009, ALICE-INT-2009-044.
[34] ALICE Collaboration, G. Chabratova, et al., Development of the Kalman Filter for Tracking in the Forward Muon Spectrometer of ALICE, 2003, ALICE-INT-2003-002.
[35] ALICE Collaboration, Supplemental figures for "ϕ-Meson production at forward rapidity in p–Pb collisions at $\sqrt{s_{NN}} = 5.02$ TeV and in pp collisions at $\sqrt{s} = 2.76$ TeV", https://cds.cern.ch/record/2195308.
[36] T. Sjostrand, S. Mrenna, P.Z. Skands, PYTHIA 6.4 physics and manual, J. High Energy Phys. 0605 (2006) 026, arXiv:hep-ph/0603175.
[37] R. Brun, F. Carminati, S. Giani, GEANT Detector Description and Simulation Tool, CERN-W-5013, 1994.
[38] Particle Data Group Collaboration, J. Beringer, et al., Review of Particle Physics (RPP), Phys. Rev. D 86 (2012) 010001.
[39] M. Oreglia, A Study of the Reactions $\psi' \to \gamma\gamma\psi$, PhD thesis, SLAC, 1980, http://search.proquest.com/docview/303036283.
[40] ALICE Collaboration, K. Aamodt, et al., Rapidity and transverse momentum dependence of inclusive J/ψ production in pp collisions at $\sqrt{s} = 7$ TeV, Phys. Lett. B 704 (2011) 442–455, arXiv:1105.0380 [hep-ex];
ALICE Collaboration, K. Aamodt, et al., Phys. Lett. B 718 (2012) 692 (Erratum).
[41] R. Barlow, Systematic errors: facts and fictions, arXiv:hep-ex/0207026.
[42] R. Engel, J. Ranft, Hadronic photon–photon interactions at high-energies, Phys. Rev. D 54 (1996) 4244–4262, arXiv:hep-ph/9509373.
[43] P.Z. Skands, Tuning Monte Carlo generators: the Perugia tunes, Phys. Rev. D 82 (2010) 074018, arXiv:1005.3457 [hep-ph].
[44] C. Buttar, D. Clements, I. Dawson, A. Moraes, Simulations of minimum bias events and the underlying event, MC tuning and predictions for the LHC, Acta Phys. Pol. B 35 (2004) 433–441.
[45] R. Field, Physics at the Tevatron, Acta Phys. Pol. B 39 (2008) 2611–2672.
[46] ALICE Collaboration, B. Abelev, et al., Production of $K^*(892)^0$ and $\phi(1020)$ in pp collisions at $\sqrt{s} = 7$ TeV, Eur. Phys. J. C 72 (2012) 2183, arXiv:1208.5717 [hep-ex].
[47] CMS Collaboration, S. Chatrchyan, et al., Study of the inclusive production of charged pions, kaons, and protons in pp collisions at $\sqrt{s} = 0.9$, 2.76, and 7 TeV, Eur. Phys. J. C 72 (2012) 2164, arXiv:1207.4724 [hep-ex].
[48] C. Tsallis, Possible generalization of Boltzmann–Gibbs statistics, J. Stat. Phys. 52 (1988) 479–487.
[49] X.-N. Wang, M. Gyulassy, HIJING: a Monte Carlo model for multiple jet production in pp, pA and AA collisions, Phys. Rev. D 44 (1991) 3501–3516.
[50] S. Roesler, R. Engel, J. Ranft, The Monte Carlo event generator DPMJET-III, in: Advanced Monte Carlo for Radiation Physics, Particle Transport Simulation and Applications. Proceedings, Conference, MC2000, Lisbon, Portugal, October 23–26, 2000, 2000, pp. 1033–1038, arXiv:hep-ph/0012252, http://www-public.slac.stanford.edu/sciDoc/docMeta.aspx?slacPubNumber=SLAC-PUB-8740.
[51] ALICE Collaboration, J. Adam, et al., Production of $K^*(892)^0$ and $\phi(1020)$ in p–Pb collisions at $\sqrt{s_{NN}} = 5.02$ TeV, Eur. Phys. J. C 76 (5) (2016) 245, arXiv:1601.07868 [nucl-ex].
[52] ALICE, LHCb Collaboration, Reference pp cross-sections for J/ψ studies in proton–lead collisions at $\sqrt{s_{NN}} = 5.02$ TeV and comparisons between ALICE and LHCb results, http://cds.cern.ch/record/1639617, CONF-2013-013.
[53] HERA-B Collaboration, I. Abt, et al., K^{*0} and ϕ meson production in proton–nucleus interactions at $\sqrt{s} = 41.6$ GeV, Eur. Phys. J. C 50 (2007) 315–328, arXiv:hep-ex/0606049.
[54] PHENIX Collaboration, A. Adare, et al., ϕ meson production in d+Au collisions at $\sqrt{s_{NN}} = 200$ GeV, Phys. Rev. C 92 (4) (2015) 044909, arXiv:1506.08181 [nucl-ex].

The ALICE Collaboration

J. Adam [40], D. Adamová [83], M.M. Aggarwal [87], G. Aglieri Rinella [36], M. Agnello [111], N. Agrawal [48], Z. Ahammed [132], S.U. Ahn [68], I. Aimo [94,111], S. Aiola [136], M. Ajaz [16], A. Akindinov [58], S.N. Alam [132], D. Aleksandrov [100], B. Alessandro [111], D. Alexandre [102], R. Alfaro Molina [64], A. Alici [105,12], A. Alkin [3], J.R.M. Almaraz [119], J. Alme [38], T. Alt [43], S. Altinpinar [18], I. Altsybeev [131], C. Alves Garcia Prado [120], C. Andrei [78], A. Andronic [97], V. Anguelov [93], J. Anielski [54], T. Antičić [98], F. Antinori [108], P. Antonioli [105], L. Aphecetche [113], H. Appelshäuser [53], S. Arcelli [28], N. Armesto [17], R. Arnaldi [111], I.C. Arsene [22], M. Arslandok [53], B. Audurier [113], A. Augustinus [36], R. Averbeck [97], M.D. Azmi [19], M. Bach [43], A. Badalà [107], Y.W. Baek [44], S. Bagnasco [111], R. Bailhache [53], R. Bala [90], A. Baldisseri [15], F. Baltasar Dos Santos Pedrosa [36], R.C. Baral [61], A.M. Barbano [111], R. Barbera [29], F. Barile [33], G.G. Barnaföldi [135], L.S. Barnby [102], V. Barret [70], P. Bartalini [7], K. Barth [36], J. Bartke [117], E. Bartsch [53], M. Basile [28], N. Bastid [70], S. Basu [132], B. Bathen [54], G. Batigne [113], A. Batista Camejo [70], B. Batyunya [66], P.C. Batzing [22], I.G. Bearden [80], H. Beck [53], C. Bedda [111], N.K. Behera [48,49], I. Belikov [55], F. Bellini [28], H. Bello Martinez [2], R. Bellwied [122], R. Belmont [134], E. Belmont-Moreno [64], V. Belyaev [76], G. Bencedi [135], S. Beole [27], I. Berceanu [78], A. Bercuci [78], Y. Berdnikov [85], D. Berenyi [135], R.A. Bertens [57], D. Berzano [36,27], L. Betev [36], A. Bhasin [90], I.R. Bhat [90], A.K. Bhati [87], B. Bhattacharjee [45], J. Bhom [128], L. Bianchi [122], N. Bianchi [72], C. Bianchin [134,57], J. Bielčík [40], J. Bielčíková [83], A. Bilandzic [80], R. Biswas [4], S. Biswas [79], S. Bjelogrlic [57], J.T. Blair [118], F. Blanco [10], D. Blau [100], C. Blume [53], F. Bock [93,74], A. Bogdanov [76], H. Bøggild [80], L. Boldizsár [135], M. Bombara [41], J. Book [53], H. Borel [15], A. Borissov [96], M. Borri [82], F. Bossú [65], E. Botta [27], S. Böttger [52], P. Braun-Munzinger [97], M. Bregant [120], T. Breitner [52], T.A. Broker [53], T.A. Browning [95], M. Broz [40], E.J. Brucken [46], E. Bruna [111], G.E. Bruno [33], D. Budnikov [99], H. Buesching [53], S. Bufalino [27,111], P. Buncic [36], O. Busch [128,93], Z. Buthelezi [65], J.B. Butt [16], J.T. Buxton [20], D. Caffarri [36], X. Cai [7], H. Caines [136],

L. Calero Diaz [72], A. Caliva [57], E. Calvo Villar [103], P. Camerini [26], F. Carena [36], W. Carena [36], F. Carnesecchi [28], J. Castillo Castellanos [15], A.J. Castro [125], E.A.R. Casula [25], C. Cavicchioli [36], C. Ceballos Sanchez [9], J. Cepila [40], P. Cerello [111], J. Cerkala [115], B. Chang [123], S. Chapeland [36], M. Chartier [124], J.L. Charvet [15], S. Chattopadhyay [132], S. Chattopadhyay [101], V. Chelnokov [3], M. Cherney [86], C. Cheshkov [130], B. Cheynis [130], V. Chibante Barroso [36], D.D. Chinellato [121], P. Chochula [36], K. Choi [96], M. Chojnacki [80], S. Choudhury [132], P. Christakoglou [81], C.H. Christensen [80], P. Christiansen [34], T. Chujo [128], S.U. Chung [96], Z. Chunhui [57], C. Cicalo [106], L. Cifarelli [12,28], F. Cindolo [105], J. Cleymans [89], F. Colamaria [33], D. Colella [36,33,59], A. Collu [25], M. Colocci [28], G. Conesa Balbastre [71], Z. Conesa del Valle [51], M.E. Connors [136], J.G. Contreras [11,40], T.M. Cormier [84], Y. Corrales Morales [27], I. Cortés Maldonado [2], P. Cortese [32], M.R. Cosentino [120], F. Costa [36], P. Crochet [70], R. Cruz Albino [11], E. Cuautle [63], L. Cunqueiro [36], T. Dahms [92,37], A. Dainese [108], A. Danu [62], D. Das [101], I. Das [101,51], S. Das [4], A. Dash [121], S. Dash [48], S. De [120], A. De Caro [31,12], G. de Cataldo [104], J. de Cuveland [43], A. De Falco [25], D. De Gruttola [12,31], N. De Marco [111], S. De Pasquale [31], A. Deisting [97,93], A. Deloff [77], E. Dénes [135,i], G. D'Erasmo [33], D. Di Bari [33], A. Di Mauro [36], P. Di Nezza [72], M.A. Diaz Corchero [10], T. Dietel [89], P. Dillenseger [53], R. Divià [36], Ø. Djuvsland [18], A. Dobrin [57,81], T. Dobrowolski [77,i], D. Domenicis Gimenez [120], B. Dönigus [53], O. Dordic [22], T. Drozhzhova [53], A.K. Dubey [132], A. Dubla [57], L. Ducroux [130], P. Dupieux [70], R.J. Ehlers [136], D. Elia [104], H. Engel [52], B. Erazmus [36,113], I. Erdemir [53], F. Erhardt [129], D. Eschweiler [43], B. Espagnon [51], M. Estienne [113], S. Esumi [128], J. Eum [96], D. Evans [102], S. Evdokimov [112], G. Eyyubova [40], L. Fabbietti [37,92], D. Fabris [108], J. Faivre [71], A. Fantoni [72], M. Fasel [74], L. Feldkamp [54], D. Felea [62], A. Feliciello [111], G. Feofilov [131], J. Ferencei [83], A. Fernández Téllez [2], E.G. Ferreiro [17], A. Ferretti [27], A. Festanti [30], V.J.G. Feuillard [15,70], J. Figiel [117], M.A.S. Figueredo [124,120], S. Filchagin [99], D. Finogeev [56], F.M. Fionda [25], E.M. Fiore [33], M.G. Fleck [93], M. Floris [36], S. Foertsch [65], P. Foka [97], S. Fokin [100], E. Fragiacomo [110], A. Francescon [36,30], U. Frankenfeld [97], U. Fuchs [36], C. Furget [71], A. Furs [56], M. Fusco Girard [31], J.J. Gaardhøje [80], M. Gagliardi [27], A.M. Gago [103], M. Gallio [27], D.R. Gangadharan [74], P. Ganoti [88], C. Gao [7], C. Garabatos [97], E. Garcia-Solis [13], C. Gargiulo [36], P. Gasik [92,37], M. Germain [113], A. Gheata [36], M. Gheata [62,36], P. Ghosh [132], S.K. Ghosh [4], P. Gianotti [72], P. Giubellino [36,111], P. Giubilato [30], E. Gladysz-Dziadus [117], P. Glässel [93], D.M. Goméz Coral [64], A. Gomez Ramirez [52], P. González-Zamora [10], S. Gorbunov [43], L. Görlich [117], S. Gotovac [116], V. Grabski [64], L.K. Graczykowski [133], K.L. Graham [102], A. Grelli [57], A. Grigoras [36], C. Grigoras [36], V. Grigoriev [76], A. Grigoryan [1], S. Grigoryan [66], B. Grinyov [3], N. Grion [110], J.F. Grosse-Oetringhaus [36], J-Y. Grossiord [130], R. Grosso [36], F. Guber [56], R. Guernane [71], B. Guerzoni [28], K. Gulbrandsen [80], H. Gulkanyan [1], T. Gunji [127], A. Gupta [90], R. Gupta [90], R. Haake [54], Ø. Haaland [18], C. Hadjidakis [51], M. Haiduc [62], H. Hamagaki [127], G. Hamar [135], A. Hansen [80], J.W. Harris [136], H. Hartmann [43], A. Harton [13], D. Hatzifotiadou [105], S. Hayashi [127], S.T. Heckel [53], M. Heide [54], H. Helstrup [38], A. Herghelegiu [78], G. Herrera Corral [11], B.A. Hess [35], K.F. Hetland [38], T.E. Hilden [46], H. Hillemanns [36], B. Hippolyte [55], R. Hosokawa [128], P. Hristov [36], M. Huang [18], T.J. Humanic [20], N. Hussain [45], T. Hussain [19], D. Hutter [43], D.S. Hwang [21], R. Ilkaev [99], I. Ilkiv [77], M. Inaba [128], M. Ippolitov [76,100], M. Irfan [19], M. Ivanov [97], V. Ivanov [85], V. Izucheev [112], P.M. Jacobs [74], S. Jadlovska [115], C. Jahnke [120], H.J. Jang [68], M.A. Janik [133], P.H.S.Y. Jayarathna [122], C. Jena [30], S. Jena [122], R.T. Jimenez Bustamante [97], P.G. Jones [102], H. Jung [44], A. Jusko [102], P. Kalinak [59], A. Kalweit [36], J. Kamin [53], J.H. Kang [137], V. Kaplin [76], S. Kar [132], A. Karasu Uysal [69], O. Karavichev [56], T. Karavicheva [56], L. Karayan [93,97], E. Karpechev [56], U. Kebschull [52], R. Keidel [138], D.L.D. Keijdener [57], M. Keil [36], K.H. Khan [16], M.M. Khan [19], P. Khan [101], S.A. Khan [132], A. Khanzadeev [85], Y. Kharlov [112], B. Kileng [38], B. Kim [137], D.W. Kim [44,68], D.J. Kim [123], H. Kim [137], J.S. Kim [44], M. Kim [44], M. Kim [137], S. Kim [21], T. Kim [137], S. Kirsch [43], I. Kisel [43], S. Kiselev [58], A. Kisiel [133], G. Kiss [135], J.L. Klay [6], C. Klein [53], J. Klein [36,93], C. Klein-Bösing [54], A. Kluge [36], M.L. Knichel [93], A.G. Knospe [118], T. Kobayashi [128], C. Kobdaj [114], M. Kofarago [36], T. Kollegger [97,43], A. Kolojvari [131], V. Kondratiev [131], N. Kondratyeva [76], E. Kondratyuk [112], A. Konevskikh [56], M. Kopcik [115], M. Kour [90], C. Kouzinopoulos [36], O. Kovalenko [77], V. Kovalenko [131], M. Kowalski [117], G. Koyithatta Meethaleveedu [48], J. Kral [123], I. Králik [59], A. Kravčáková [41], M. Kretz [43], M. Krivda [59,102], F. Krizek [83], E. Kryshen [36], M. Krzewicki [43], A.M. Kubera [20], V. Kučera [83], T. Kugathasan [36], C. Kuhn [55], P.G. Kuijer [81], A. Kumar [90], J. Kumar [48], L. Kumar [79,87], P. Kurashvili [77], A. Kurepin [56], A.B. Kurepin [56], A. Kuryakin [99], S. Kushpil [83], M.J. Kweon [50], Y. Kwon [137], S.L. La Pointe [111], P. La Rocca [29], C. Lagana Fernandes [120], I. Lakomov [36], R. Langoy [42], C. Lara [52], A. Lardeux [15], A. Lattuca [27], E. Laudi [36],

R. Lea [26], L. Leardini [93], G.R. Lee [102], S. Lee [137], I. Legrand [36], F. Lehas [81], R.C. Lemmon [82], V. Lenti [104], E. Leogrande [57], I. León Monzón [119], M. Leoncino [27], P. Lévai [135], S. Li [7,70], X. Li [14], J. Lien [42], R. Lietava [102], S. Lindal [22], V. Lindenstruth [43], C. Lippmann [97], M.A. Lisa [20], H.M. Ljunggren [34], D.F. Lodato [57], P.I. Loenne [18], V. Loginov [76], C. Loizides [74], X. Lopez [70], E. López Torres [9], A. Lowe [135], P. Luettig [53], M. Lunardon [30], G. Luparello [26], P.H.F.N.D. Luz [120], A. Maevskaya [56], M. Mager [36], S. Mahajan [90], S.M. Mahmood [22], A. Maire [55], R.D. Majka [136], M. Malaev [85], I. Maldonado Cervantes [63], L. Malinina [66,ii], D. Mal'Kevich [58], P. Malzacher [97], A. Mamonov [99], V. Manko [100], F. Manso [70], V. Manzari [36,104], M. Marchisone [27], J. Mareš [60], G.V. Margagliotti [26], A. Margotti [105], J. Margutti [57], A. Marín [97], C. Markert [118], M. Marquard [53], N.A. Martin [97], J. Martin Blanco [113], P. Martinengo [36], M.I. Martínez [2], G. Martínez García [113], M. Martinez Pedreira [36], Y. Martynov [3], A. Mas [120], S. Masciocchi [97], M. Masera [27], A. Masoni [106], L. Massacrier [113], A. Mastroserio [33], H. Masui [128], A. Matyja [117], C. Mayer [117], J. Mazer [125], M.A. Mazzoni [109], D. Mcdonald [122], F. Meddi [24], Y. Melikyan [76], A. Menchaca-Rocha [64], E. Meninno [31], J. Mercado Pérez [93], M. Meres [39], Y. Miake [128], M.M. Mieskolainen [46], K. Mikhaylov [66,58], L. Milano [36], J. Milosevic [22], L.M. Minervini [104,23], A. Mischke [57], A.N. Mishra [49], D. Miśkowiec [97], J. Mitra [132], C.M. Mitu [62], N. Mohammadi [57], B. Mohanty [132,79], L. Molnar [55], L. Montaño Zetina [11], E. Montes [10], M. Morando [30], D.A. Moreira De Godoy [113,54], S. Moretto [30], A. Morreale [113], A. Morsch [36], V. Muccifora [72], E. Mudnic [116], D. Mühlheim [54], S. Muhuri [132], M. Mukherjee [132], J.D. Mulligan [136], M.G. Munhoz [120], S. Murray [65], L. Musa [36], J. Musinsky [59], B.K. Nandi [48], R. Nania [105], E. Nappi [104], M.U. Naru [16], C. Nattrass [125], K. Nayak [79], T.K. Nayak [132], S. Nazarenko [99], A. Nedosekin [58], L. Nellen [63], F. Ng [122], M. Nicassio [97], M. Niculescu [62,36], J. Niedziela [36], B.S. Nielsen [80], S. Nikolaev [100], S. Nikulin [100], V. Nikulin [85], F. Noferini [105,12], P. Nomokonov [66], G. Nooren [57], J.C.C. Noris [2], J. Norman [124], A. Nyanin [100], J. Nystrand [18], H. Oeschler [93], S. Oh [136], S.K. Oh [67], A. Ohlson [36], A. Okatan [69], T. Okubo [47], L. Olah [135], J. Oleniacz [133], A.C. Oliveira Da Silva [120], M.H. Oliver [136], J. Onderwaater [97], C. Oppedisano [111], R. Orava [46], A. Ortiz Velasquez [63], A. Oskarsson [34], J. Otwinowski [117], K. Oyama [93], M. Ozdemir [53], Y. Pachmayer [93], P. Pagano [31], G. Paić [63], C. Pajares [17], S.K. Pal [132], J. Pan [134], A.K. Pandey [48], D. Pant [48], P. Papcun [115], V. Papikyan [1], G.S. Pappalardo [107], P. Pareek [49], W.J. Park [97], S. Parmar [87], A. Passfeld [54], V. Paticchio [104], R.N. Patra [132], B. Paul [101], T. Peitzmann [57], H. Pereira Da Costa [15], E. Pereira De Oliveira Filho [120], D. Peresunko [100,76], C.E. Pérez Lara [81], E. Perez Lezama [53], V. Peskov [53], Y. Pestov [5], V. Petráček [40], V. Petrov [112], M. Petrovici [78], C. Petta [29], S. Piano [110], M. Pikna [39], P. Pillot [113], O. Pinazza [105,36], L. Pinsky [122], D.B. Piyarathna [122], M. Płoskoń [74], M. Planinic [129], J. Pluta [133], S. Pochybova [135], P.L.M. Podesta-Lerma [119], M.G. Poghosyan [86,84], B. Polichtchouk [112], N. Poljak [129], W. Poonsawat [114], A. Pop [78], S. Porteboeuf-Houssais [70], J. Porter [74], J. Pospisil [83], S.K. Prasad [4], R. Preghenella [36,105], F. Prino [111], C.A. Pruneau [134], I. Pshenichnov [56], M. Puccio [111], G. Puddu [25], P. Pujahari [134], V. Punin [99], J. Putschke [134], H. Qvigstad [22], A. Rachevski [110], S. Raha [4], S. Rajput [90], J. Rak [123], A. Rakotozafindrabe [15], L. Ramello [32], F. Rami [55], R. Raniwala [91], S. Raniwala [91], S.S. Räsänen [46], B.T. Rascanu [53], D. Rathee [87], K.F. Read [125], J.S. Real [71], K. Redlich [77], R.J. Reed [134], A. Rehman [18], P. Reichelt [53], F. Reidt [93,36], X. Ren [7], R. Renfordt [53], A.R. Reolon [72], A. Reshetin [56], F. Rettig [43], J-P. Revol [12], K. Reygers [93], V. Riabov [85], R.A. Ricci [73], T. Richert [34], M. Richter [22], P. Riedler [36], W. Riegler [36], F. Riggi [29], C. Ristea [62], A. Rivetti [111], E. Rocco [57], M. Rodríguez Cahuantzi [2], A. Rodriguez Manso [81], K. Røed [22], E. Rogochaya [66], D. Rohr [43], D. Röhrich [18], R. Romita [124], F. Ronchetti [72], L. Ronflette [113], P. Rosnet [70], A. Rossi [30,36], F. Roukoutakis [88], A. Roy [49], C. Roy [55], P. Roy [101], A.J. Rubio Montero [10], R. Rui [26], R. Russo [27], E. Ryabinkin [100], Y. Ryabov [85], A. Rybicki [117], S. Sadovsky [112], K. Šafařík [36], B. Sahlmuller [53], P. Sahoo [49], R. Sahoo [49], S. Sahoo [61], P.K. Sahu [61], J. Saini [132], S. Sakai [72], M.A. Saleh [134], C.A. Salgado [17], J. Salzwedel [20], S. Sambyal [90], V. Samsonov [85], X. Sanchez Castro [55], L. Šándor [59], A. Sandoval [64], M. Sano [128], D. Sarkar [132], E. Scapparone [105], F. Scarlassara [30], R.P. Scharenberg [95], C. Schiaua [78], R. Schicker [93], C. Schmidt [97], H.R. Schmidt [35], S. Schuchmann [53], J. Schukraft [36], M. Schulc [40], T. Schuster [136], Y. Schutz [113,36], K. Schwarz [97], K. Schweda [97], G. Scioli [28], E. Scomparin [111], R. Scott [125], J.E. Seger [86], Y. Sekiguchi [127], D. Sekihata [47], I. Selyuzhenkov [97], K. Senosi [65], J. Seo [96,67], E. Serradilla [64,10], A. Sevcenco [62], A. Shabanov [56], A. Shabetai [113], O. Shadura [3], R. Shahoyan [36], A. Shangaraev [112], A. Sharma [90], M. Sharma [90], M. Sharma [90], N. Sharma [125,61], K. Shigaki [47], K. Shtejer [9,27], Y. Sibiriak [100], S. Siddhanta [106], K.M. Sielewicz [36], T. Siemiarczuk [77], D. Silvermyr [84,34], C. Silvestre [71], G. Simatovic [129], G. Simonetti [36], R. Singaraju [132], R. Singh [79], S. Singha [132,79], V. Singhal [132], B.C. Sinha [132], T. Sinha [101], B. Sitar [39],

M. Sitta [32], T.B. Skaali [22], M. Slupecki [123], N. Smirnov [136], R.J.M. Snellings [57], T.W. Snellman [123], C. Søgaard [34], R. Soltz [75], J. Song [96], M. Song [137], Z. Song [7], F. Soramel [30], S. Sorensen [125], M. Spacek [40], E. Spiriti [72], I. Sputowska [117], M. Spyropoulou-Stassinaki [88], B.K. Srivastava [95], J. Stachel [93], I. Stan [62], G. Stefanek [77], M. Steinpreis [20], E. Stenlund [34], G. Steyn [65], J.H. Stiller [93], D. Stocco [113], P. Strmen [39], A.A.P. Suaide [120], T. Sugitate [47], C. Suire [51], M. Suleymanov [16], R. Sultanov [58], M. Šumbera [83], T.J.M. Symons [74], A. Szabo [39], A. Szanto de Toledo [120,i], I. Szarka [39], A. Szczepankiewicz [36], M. Szymanski [133], U. Tabassam [16], J. Takahashi [121], G.J. Tambave [18], N. Tanaka [128], M.A. Tangaro [33], J.D. Tapia Takaki [51,iii], A. Tarantola Peloni [53], M. Tarhini [51], M. Tariq [19], M.G. Tarzila [78], A. Tauro [36], G. Tejeda Muñoz [2], A. Telesca [36], K. Terasaki [127], C. Terrevoli [30,25], B. Teyssier [130], J. Thäder [74,97], D. Thomas [118], R. Tieulent [130], A.R. Timmins [122], A. Toia [53], S. Trogolo [111], V. Trubnikov [3], W.H. Trzaska [123], T. Tsuji [127], A. Tumkin [99], R. Turrisi [108], T.S. Tveter [22], K. Ullaland [18], A. Uras [130], G.L. Usai [25], A. Utrobicic [129], M. Vajzer [83], M. Vala [59], L. Valencia Palomo [70], S. Vallero [27], J. Van Der Maarel [57], J.W. Van Hoorne [36], M. van Leeuwen [57], T. Vanat [83], P. Vande Vyvre [36], D. Varga [135], A. Vargas [2], M. Vargyas [123], R. Varma [48], M. Vasileiou [88], A. Vasiliev [100], A. Vauthier [71], V. Vechernin [131], A.M. Veen [57], M. Veldhoen [57], A. Velure [18], M. Venaruzzo [73], E. Vercellin [27], S. Vergara Limón [2], R. Vernet [8], M. Verweij [134,36], L. Vickovic [116], G. Viesti [30,i], J. Viinikainen [123], Z. Vilakazi [126], O. Villalobos Baillie [102], A. Vinogradov [100], L. Vinogradov [131], Y. Vinogradov [99,i], T. Virgili [31], V. Vislavicius [34], Y.P. Viyogi [132], A. Vodopyanov [66], M.A. Völkl [93], K. Voloshin [58], S.A. Voloshin [134], G. Volpe [135,36], B. von Haller [36], I. Vorobyev [37,92], D. Vranic [36,97], J. Vrláková [41], B. Vulpescu [70], A. Vyushin [99], B. Wagner [18], J. Wagner [97], H. Wang [57], M. Wang [7,113], Y. Wang [93], D. Watanabe [128], Y. Watanabe [127], M. Weber [36], S.G. Weber [97], J.P. Wessels [54], U. Westerhoff [54], J. Wiechula [35], J. Wikne [22], M. Wilde [54], G. Wilk [77], J. Wilkinson [93], M.C.S. Williams [105], B. Windelband [93], M. Winn [93], C.G. Yaldo [134], H. Yang [57], P. Yang [7], S. Yano [47], Z. Yin [7], H. Yokoyama [128], I-K. Yoo [96], V. Yurchenko [3], I. Yushmanov [100], A. Zaborowska [133], V. Zaccolo [80], A. Zaman [16], C. Zampolli [105], H.J.C. Zanoli [120], S. Zaporozhets [66], N. Zardoshti [102], A. Zarochentsev [131], P. Závada [60], N. Zaviyalov [99], H. Zbroszczyk [133], I.S. Zgura [62], M. Zhalov [85], H. Zhang [18,7], X. Zhang [74], Y. Zhang [7], C. Zhao [22], N. Zhigareva [58], D. Zhou [7], Y. Zhou [80,57], Z. Zhou [18], H. Zhu [18,7], J. Zhu [7,113], X. Zhu [7], A. Zichichi [28,12], A. Zimmermann [93], M.B. Zimmermann [36,54], G. Zinovjev [3], M. Zyzak [43]

[1] *A.I. Alikhanyan National Science Laboratory (Yerevan Physics Institute) Foundation, Yerevan, Armenia*
[2] *Benemérita Universidad Autónoma de Puebla, Puebla, Mexico*
[3] *Bogolyubov Institute for Theoretical Physics, Kiev, Ukraine*
[4] *Bose Institute, Department of Physics and Centre for Astroparticle Physics and Space Science (CAPSS), Kolkata, India*
[5] *Budker Institute for Nuclear Physics, Novosibirsk, Russia*
[6] *California Polytechnic State University, San Luis Obispo, CA, United States*
[7] *Central China Normal University, Wuhan, China*
[8] *Centre de Calcul de l'IN2P3, Villeurbanne, France*
[9] *Centro de Aplicaciones Tecnológicas y Desarrollo Nuclear (CEADEN), Havana, Cuba*
[10] *Centro de Investigaciones Energéticas Medioambientales y Tecnológicas (CIEMAT), Madrid, Spain*
[11] *Centro de Investigación y de Estudios Avanzados (CINVESTAV), Mexico City and Mérida, Mexico*
[12] *Centro Fermi – Museo Storico della Fisica e Centro Studi e Ricerche "Enrico Fermi", Rome, Italy*
[13] *Chicago State University, Chicago, IL, United States*
[14] *China Institute of Atomic Energy, Beijing, China*
[15] *Commissariat à l'Energie Atomique, IRFU, Saclay, France*
[16] *COMSATS Institute of Information Technology (CIIT), Islamabad, Pakistan*
[17] *Departamento de Física de Partículas and IGFAE, Universidad de Santiago de Compostela, Santiago de Compostela, Spain*
[18] *Department of Physics and Technology, University of Bergen, Bergen, Norway*
[19] *Department of Physics, Aligarh Muslim University, Aligarh, India*
[20] *Department of Physics, Ohio State University, Columbus, OH, United States*
[21] *Department of Physics, Sejong University, Seoul, South Korea*
[22] *Department of Physics, University of Oslo, Oslo, Norway*
[23] *Dipartimento di Elettrotecnica ed Elettronica del Politecnico, Bari, Italy*
[24] *Dipartimento di Fisica dell'Università 'La Sapienza' and Sezione INFN Rome, Italy*
[25] *Dipartimento di Fisica dell'Università and Sezione INFN, Cagliari, Italy*
[26] *Dipartimento di Fisica dell'Università and Sezione INFN, Trieste, Italy*
[27] *Dipartimento di Fisica dell'Università and Sezione INFN, Turin, Italy*
[28] *Dipartimento di Fisica e Astronomia dell'Università and Sezione INFN, Bologna, Italy*
[29] *Dipartimento di Fisica e Astronomia dell'Università and Sezione INFN, Catania, Italy*
[30] *Dipartimento di Fisica e Astronomia dell'Università and Sezione INFN, Padova, Italy*
[31] *Dipartimento di Fisica 'E.R. Caianiello' dell'Università and Gruppo Collegato INFN, Salerno, Italy*
[32] *Dipartimento di Scienze e Innovazione Tecnologica dell'Università del Piemonte Orientale and Gruppo Collegato INFN, Alessandria, Italy*
[33] *Dipartimento Interateneo di Fisica 'M. Merlin' and Sezione INFN, Bari, Italy*
[34] *Division of Experimental High Energy Physics, University of Lund, Lund, Sweden*
[35] *Eberhard Karls Universität Tübingen, Tübingen, Germany*
[36] *European Organization for Nuclear Research (CERN), Geneva, Switzerland*
[37] *Excellence Cluster Universe, Technische Universität München, Munich, Germany*

[38] Faculty of Engineering, Bergen University College, Bergen, Norway
[39] Faculty of Mathematics, Physics and Informatics, Comenius University, Bratislava, Slovakia
[40] Faculty of Nuclear Sciences and Physical Engineering, Czech Technical University in Prague, Prague, Czechia
[41] Faculty of Science, P.J. Šafárik University, Košice, Slovakia
[42] Faculty of Technology, Buskerud and Vestfold University College, Vestfold, Norway
[43] Frankfurt Institute for Advanced Studies, Johann Wolfgang Goethe-Universität Frankfurt, Frankfurt, Germany
[44] Gangneung-Wonju National University, Gangneung, South Korea
[45] Gauhati University, Department of Physics, Guwahati, India
[46] Helsinki Institute of Physics (HIP), Helsinki, Finland
[47] Hiroshima University, Hiroshima, Japan
[48] Indian Institute of Technology Bombay (IIT), Mumbai, India
[49] Indian Institute of Technology Indore, Indore (IITI), India
[50] Inha University, Incheon, South Korea
[51] Institut de Physique Nucléaire d'Orsay (IPNO), Université Paris-Sud, CNRS-IN2P3, Orsay, France
[52] Institut für Informatik, Johann Wolfgang Goethe-Universität Frankfurt, Frankfurt, Germany
[53] Institut für Kernphysik, Johann Wolfgang Goethe-Universität Frankfurt, Frankfurt, Germany
[54] Institut für Kernphysik, Westfälische Wilhelms-Universität Münster, Münster, Germany
[55] Institut Pluridisciplinaire Hubert Curien (IPHC), Université de Strasbourg, CNRS-IN2P3, Strasbourg, France
[56] Institute for Nuclear Research, Academy of Sciences, Moscow, Russia
[57] Institute for Subatomic Physics of Utrecht University, Utrecht, Netherlands
[58] Institute for Theoretical and Experimental Physics, Moscow, Russia
[59] Institute of Experimental Physics, Slovak Academy of Sciences, Košice, Slovakia
[60] Institute of Physics, Academy of Sciences of the Czech Republic, Prague, Czechia
[61] Institute of Physics, Bhubaneswar, India
[62] Institute of Space Science (ISS), Bucharest, Romania
[63] Instituto de Ciencias Nucleares, Universidad Nacional Autónoma de México, Mexico City, Mexico
[64] Instituto de Física, Universidad Nacional Autónoma de México, Mexico City, Mexico
[65] iThemba LABS, National Research Foundation, Somerset West, South Africa
[66] Joint Institute for Nuclear Research (JINR), Dubna, Russia
[67] Konkuk University, Seoul, South Korea
[68] Korea Institute of Science and Technology Information, Daejeon, South Korea
[69] KTO Karatay University, Konya, Turkey
[70] Laboratoire de Physique Corpusculaire (LPC), Clermont Université, Université Blaise Pascal, CNRS-IN2P3, Clermont-Ferrand, France
[71] Laboratoire de Physique Subatomique et de Cosmologie, Université Grenoble-Alpes, CNRS-IN2P3, Grenoble, France
[72] Laboratori Nazionali di Frascati, INFN, Frascati, Italy
[73] Laboratori Nazionali di Legnaro, INFN, Legnaro, Italy
[74] Lawrence Berkeley National Laboratory, Berkeley, CA, United States
[75] Lawrence Livermore National Laboratory, Livermore, CA, United States
[76] Moscow Engineering Physics Institute, Moscow, Russia
[77] National Centre for Nuclear Studies, Warsaw, Poland
[78] National Institute for Physics and Nuclear Engineering, Bucharest, Romania
[79] National Institute of Science Education and Research, Bhubaneswar, India
[80] Niels Bohr Institute, University of Copenhagen, Copenhagen, Denmark
[81] Nikhef, Nationaal instituut voor subatomaire fysica, Amsterdam, Netherlands
[82] Nuclear Physics Group, STFC Daresbury Laboratory, Daresbury, United Kingdom
[83] Nuclear Physics Institute, Academy of Sciences of the Czech Republic, Řež u Prahy, Czechia
[84] Oak Ridge National Laboratory, Oak Ridge, TN, United States
[85] Petersburg Nuclear Physics Institute, Gatchina, Russia
[86] Physics Department, Creighton University, Omaha, NE, United States
[87] Physics Department, Panjab University, Chandigarh, India
[88] Physics Department, University of Athens, Athens, Greece
[89] Physics Department, University of Cape Town, Cape Town, South Africa
[90] Physics Department, University of Jammu, Jammu, India
[91] Physics Department, University of Rajasthan, Jaipur, India
[92] Physik Department, Technische Universität München, Munich, Germany
[93] Physikalisches Institut, Ruprecht-Karls-Universität Heidelberg, Heidelberg, Germany
[94] Politecnico di Torino, Turin, Italy
[95] Purdue University, West Lafayette, IN, United States
[96] Pusan National University, Pusan, South Korea
[97] Research Division and ExtreMe Matter Institute EMMI, GSI Helmholtzzentrum für Schwerionenforschung, Darmstadt, Germany
[98] Rudjer Bošković Institute, Zagreb, Croatia
[99] Russian Federal Nuclear Center (VNIIEF), Sarov, Russia
[100] Russian Research Centre Kurchatov Institute, Moscow, Russia
[101] Saha Institute of Nuclear Physics, Kolkata, India
[102] School of Physics and Astronomy, University of Birmingham, Birmingham, United Kingdom
[103] Sección Física, Departamento de Ciencias, Pontificia Universidad Católica del Perú, Lima, Peru
[104] Sezione INFN, Bari, Italy
[105] Sezione INFN, Bologna, Italy
[106] Sezione INFN, Cagliari, Italy
[107] Sezione INFN, Catania, Italy
[108] Sezione INFN, Padova, Italy
[109] Sezione INFN, Rome, Italy
[110] Sezione INFN, Trieste, Italy
[111] Sezione INFN, Turin, Italy
[112] SSC IHEP of NRC Kurchatov institute, Protvino, Russia
[113] SUBATECH, Ecole des Mines de Nantes, Université de Nantes, CNRS-IN2P3, Nantes, France
[114] Suranaree University of Technology, Nakhon Ratchasima, Thailand
[115] Technical University of Košice, Košice, Slovakia
[116] Technical University of Split FESB, Split, Croatia

[117] The Henryk Niewodniczanski Institute of Nuclear Physics, Polish Academy of Sciences, Cracow, Poland
[118] The University of Texas at Austin, Physics Department, Austin, TX, United States
[119] Universidad Autónoma de Sinaloa, Culiacán, Mexico
[120] Universidade de São Paulo (USP), São Paulo, Brazil
[121] Universidade Estadual de Campinas (UNICAMP), Campinas, Brazil
[122] University of Houston, Houston, TX, United States
[123] University of Jyväskylä, Jyväskylä, Finland
[124] University of Liverpool, Liverpool, United Kingdom
[125] University of Tennessee, Knoxville, TN, United States
[126] University of the Witwatersrand, Johannesburg, South Africa
[127] University of Tokyo, Tokyo, Japan
[128] University of Tsukuba, Tsukuba, Japan
[129] University of Zagreb, Zagreb, Croatia
[130] Université de Lyon, Université Lyon 1, CNRS/IN2P3, IPN-Lyon, Villeurbanne, France
[131] V. Fock Institute for Physics, St. Petersburg State University, St. Petersburg, Russia
[132] Variable Energy Cyclotron Centre, Kolkata, India
[133] Warsaw University of Technology, Warsaw, Poland
[134] Wayne State University, Detroit, MI, United States
[135] Wigner Research Centre for Physics, Hungarian Academy of Sciences, Budapest, Hungary
[136] Yale University, New Haven, CT, United States
[137] Yonsei University, Seoul, South Korea
[138] Zentrum für Technologietransfer und Telekommunikation (ZTT), Fachhochschule Worms, Worms, Germany

[i] Deceased.
[ii] Also at: M.V. Lomonosov Moscow State University, D.V. Skobeltsyn Institute of Nuclear, Physics, Moscow, Russia.
[iii] Also at: University of Kansas, Lawrence, KS, United States.